Article

HISTORICAL BIOGEOGRAPHY OF THE AUSTRAL HORNWORT GENUS *PHAEOMEGACEROS* (DENDROCEROTACEAE, ANTHOCEROTOPHYTA)

GABRIEL F. PEÑALOZA-BOJACÁ[1*], ADRIEL M. SIERRA[2,3*], HANNES BECHER[4], KAREN S. RENZAGLIA[5] & JUAN CARLOS VILLARREAL A.[2,3]

[1]*Laboratório de Sistemática Vegetal, Departamento de Botânica, Universidade Federal de Minas Gerais, Brasil*
✉ *gpenaloza.bojaca@gmail.com;* ⓞ *https://orcid.org/0000-0001-7085-9521*
[2]*Département de Biologie, Université Laval, Québec, G1V 0A6, Canada*
[3]*Institut de Biologie Intégrative et dês Systèmes (IBIS), Université Laval, Québec, G1V 0A6, Canada*
✉ *adriel-michel.sierra-pinilla.1@ulaval.ca;* ⓞ *https://orcid.org/0000-0001-9900-1350*
✉ *juan-carlos.villarreal-aguilar@bio.ulaval.ca;* ⓞ *https://orcid.org/0000-0002-0770-1446*
[4]*Institute of Genetics and Cancer University of Edinburgh, Crewe Road, Edinburgh, EH9 3FL*
✉ *H.Becher@ed.ac.uk,* ⓞ *https://orcid.org/0000-0003-3700-2942*
[5]*Department of Plant Biology, Southern Illinois University, Carbondale, IL, USA*
✉ *renzaglia@plant.siu.edu;* ⓞ *https://orcid.org/0000-0002-1406-2646*
Corresponding author: Gabriel Peñaloza-Bojacá: ✉ *gpenaloza.bojaca@gmail.com*
*Equal contribution

Abstract

The transoceanic disjunct distributions between Australasia and Austral America have been observed in many plant groups. The processes behind these disjunct distributions remain a source of debate due to differences in species vagility, biogeographical history, and complex geological and climatic changes. We address the phylogenetic relationships and biogeographical history of the austral hornwort genus *Phaeomegaceros* based on eight molecular markers from the three genomes (nuclear: phytochrome, mitochondrial: *nad5*, and chloroplast: *rbcL*, *trnL* intron, *trnL-trnF* spacer, *rps4* gene, *rps4-trnS* spacer, and *matK* gene). With ten taxa based on morphological and molecular data, the three phylogenetic analyses supported the genus *Phaeomegaceros* as monophyletic. *Phaeomegaceros* is composed of two major clades corresponding to the New Zealand species, which presents a conspicuous trilete mark with one depression in the middle of the spore's proximal face, and the Austral American species, which lack this middle depression. Dating and biogeographical analyses indicate that the *Phaeomegaceros* ancestral area was New Zealand and Antarctica in the Late Cretaceous (53.51 Ma, HPD 95% = 31.64–72.63). While Austral American species diverged during the Eocene. We speculate that climatic fluctuations in the Antarctic continent during the middle to late-Miocene led to the isolation of *Phaeomegaceros* taxa with both processes (dispersal events and vicariance) acting on the independent evolution of the disjunct clades. Furthermore, recent diversification of *Phaeomegaceros* taxa in Austral America and range expansion to northern Andes and oceanic islands, are explained by dispersal events and subsequent cladogenesis coinciding with the uplift of the Andes and the formation of volcanic oceanic islands (Juan Fernandez and Tristan da Cunha).

Keywords: Antarctica, cryptogams, Gondwana, long-distance dispersal, speciation, spore morphology

Dedication

We dedicate this paper to *Jeffrey G. Duckett* whose collecting expeditions around the world and in-depth studies of morphology and plant-fungal symbioses have made important contributions to our understanding of hornwort diversity and biology.

Introduction

Vicariance and dispersal, historical processes behind the disjunct distribution of many plant lineages between Australasia (including Australia, Melanesia, and New Zealand) and Austral America (Patagonia), have remained controversial due

to differences in species vagility, biogeographical history, and complex geological and climatic changes (Linder and Crisp 1995; Hill 2001; Swenson *et al.* 2001). More realistic biogeographic ancestral area reconstruction analyses have led to a better understanding of the processes shaping the austral disjunct flora (Mao *et al.* 2012; Estrella *et al.* 2019; Vasconcelos *et al.* 2017). The two regions Australasia and Austral America were part of the supercontinent Gondwana, which start to break a part around 82 Ma (Markgraf *et al.* 1995). The derivative fragments of the former supercontinent remained connected, to varying degrees, from the Late Cretaceous to the middle Eocene (Pross *et al.* 2012), via an ice-free Antarctica that harbored a diverse evergreen forest. These forest habitats are inferred to have played a key role as a dispersal route between populations in both continents, including bryophytes (Estrella *et al.* 2019). From the late Miocene to the Last Glacial Maximum (LGM) of the Pleistocene most of the Antarctic continent became covered by ice (Gasson & Keisling 2020). The LGM isolated, formerly connected plant and animal populations across the Austral region, contributing to the disjunct distributions observed today (Estrella *et al.* 2019; Vasconcelos *et al.* 2017).

Divergence time estimates between disjunct populations on either side of the Southern Pacific Ocean recovered by time-calibrated molecular phylogenies, support ongoing connectivity between populations by long-distance dispersal (Renner *et al.* 2000, Setoguchi *et al.* 1997, Sanmartín & Ronquist 2004; Knapp *et al.* 2005). For example, the emblematic Austral tree genus *Nothofagus* Blume (1850: 307) diverged between Australasia and Austral American species around 25 Ma, significantly younger than the continental break-up, suggesting that colonization of the American continent may have occurred via transoceanic dispersal (Renner *et al.* 2000; Setoguchi *et al.* 1997; Sanmartín & Ronquist 2004; Knapp *et al.* 2005, but see Sauquet *et al.* 2012 for an assessment of the influence of time-calibration strategy on inferred divergence scenarios).

Either eastward long-distance dispersal events from New Zealand to Austral America, or a combination of dispersal and vicariance, have been inferred as shaping the disjunct geographical distribution of seed-free plants (Sanmartín *et al.* 2007; Korall & Pryer 2014; Morero *et al.* 2019), especially bryophytes and ferns (Korall & Pryer 2014; Vanderpoorten *et al.* 2010). Even though, pioneer molecular dating studies supported a vicariance scenario in bryophytes (Meißner *et al.* 1998; McDaniel & Shaw 2003), more recent studies have found high genetic similarity between Australasian and Austral American taxa (Quandt *et al.* 2001; Pfeiffer 2000; Frey *et al.* 1999; Stech *et al.* 2002). Using sophisticated ancestral area inferences, transoceanic long-distance dispersal seems to be a more likely process behind the current bryophyte distribution in both sides of the Southern Pacific Ocean (Carter *et al.* 2017; Pokorny *et al.* 2011; Sun *et al.* 2014; Vanderpoorten *et al.* 2010). In addition, fossil records identified the persistence of bryophyte species in Antarctica's cold climate long after the break-up of Gondwana (c. 65 mya; Biersma *et al.* 2018; Pisa *et al.* 2014; Lewis *et al.* 2008). The advance of ice-sheets in Antarctica during the mid-Miocene may have accelerated the extinction of tundra-associated plant communities (Lewis *et al.* 2008). The glaciers could have isolated populations once connected through the Antarctic continent. Recent evidence suggest that bryophytes regenerate long after being under the permafrost (Roads *et al.* 2014), which have supported the persistence of isolated connections between both austral continents up to the Mid-Miocene. All these confluent scenarios should be taken into account while inferring the biogeography of Austral disjunct bryophytes by assigning Antarctica as a major area of interest in biogeographic reconstructions following Estrella *et al.* (2019).

The hornwort genera *Nothoceros* (Schuster) Hasegawa (1994: 32), and *Phaeomegaceros* Duff, Villarreal, Cargill & Renzaglia (2007: 241) (Dendrocerotaceae) represent examples of bryophyte taxa with an extant disjunct distribution between the Austral geographical regions (Villarreal *et al.* 2010a). *Phaeomegaceros* is distributed across the Australasia (New Zealand and Java), and in South America up to Mexico, with several narrow endemic taxa in the Andes and oceanic islands (Duff *et al.* 2007; Villarreal *et al.* 2010a; Ibarra-Morales *et al.* 2020). Three of the ten species consider here occur in South-East Pacific Islands within Australasia, and five species in America, of which five are distributed in Austral South America. While *Phaeomegaceros fimbriatus* (Gottsche; 1864:187) Duff, Villarreal, Cargill & Renzaglia (2007: 241) is restricted to South and Central America (Duff *et al.* 2007) and *Phaeomegaceros plicatus* (Mitten; 1884: 178) Villarreal, Engel & Váňa (2013: 85) to the Atlantic Island of Tristan da Cunha (Söderström *et al.* 2016; Villarreal *et al.* 2010a; Ibarra-Morales *et al.* 2020). Taxonomic and ultrastructural studies found that all species of *Phaeomegaceros* share large solid thalli, chloroplasts lacking a pyrenoid, sporophytes with stomata, one-celled yellow spores with distal depressions or foveas, and elongated pseudoelaters (Duff *et al.* 2007; Villarreal *et al.* 2010a). However, the spore proximal face presents diagnostic differences between Australasian and American species. Within the American species the distal spore architecture can be used to delimit the species, but intraspecific variation is observed in *P. squamuliger* (Spruce; 1985: 576) Villarreal (2010b: 351) and *P. fimbriatus* (Villarreal & Renzaglia 2006, Villarreal *et al.* 2010b).

In this study, we generated a dated phylogeny based on eight molecular markers and reconstructed ancestral areas to infer the historical biogeography of nine taxa, comprising seven described and two undescribed species of

Phaeomegaceros. We explore whether the current patterns of disjunction in *Phaeomegaceros* are due to oceanic long-distance dispersal or vicariance mediated by the Antarctic region as a land bridge between continents. We test two potential scenarios. First, if the genus *Phaeomegaceros* originated in Australasia (specifically: New Zealand - NZ), a long-distance dispersal event to Austral America (Villarreal *et al.* 2015) explain the current distribution. Alternatively, if divergence times were to coincide with an ice-free Antarctica before the early Miocene (c. 12 Ma), Antarctica might have acted as a land bridge connecting the present disjunct taxa between Australasia (NZ) and Austral America species. Then, the species became separated during the glacier cover in the Miocene to Pleistocene.

TABLE 1. *Phaeomegaceros* species (in bold species included in the molecular phylogeny) with its global distribution, and description of spore distal and proximal face.

Species	Global distribution	Spore distal face	Spore proximal face
P. fimbriatus	Montane cloud forest in Central America (Costa Rica, Panamá), Andes (Colombia, Ecuador, Venezuela) and Mexico; Páramo in Central America and northern Andes	Vermiculate with five to seven foveas surrounding a central fovea	Conspicuous trilete mark with prominent triradiate ridge. Vermiculate
P. plicatus	Tristan da Cunha (Southern Atlantic Ocean)	Delicately vermiculate and shallow foveas of cingulum distinct	
P. skottsbergii	Juan Fernández Islands (Chile, Pacific Ocean)	Vermiculate, with one central large protuberant foveas, and twelve shallow foveas	Conspicuous trilete mark, slightly vermiculate
P. chiloensis	Chile	Densely vermiculate with shallow foveas	Conspicuous trilete mark, slightly vermiculate
P. squamuliger	Chile	Vermiculate slightly irregular shaped	Conspicuous trilete mark, slightly vermiculate
P. squamuliger subsp. **hasselii**	Chile		Conspicuous trilete mark, slightly vermiculate
Phaeomegaceros sp. 2	Chile	Brain-like ornamentation	Conspicuous trilete mark, with abundant vermiculate
Phaeomegaceros sp. 1	Chile	Vermiculate without foveas	Conspicuous trilete mark, slightly vermiculate
P. coriaceus	New Zealand	Eight to ten shallow dimples	Conspicuous trilete mark, with one fovea in the middle of each of the proximal facets
P. hirticalyx	New Zealand and Java	Eight to ten shallow dimples	Conspicuous trilete mark, with one fovea in the middle of each of the proximal facets (only NZ plants)
P. foveatus	Southeast Asia	Vermiculate with eight to seven foveas surrounding a central fovea	Conspicuous trilete mark, with one fovea in the middle of each of the proximal facets

Material & Methods

Taxon sampling—To address the phylogenetic relationships within *Phaeomegaceros* we included nine species of the ten known taxa (Table 1), that correspond to seven of the eight currently accepted species, and two undescribed species collected by Jeff Duckett from Chile (*Phaeomegaceros sp. 1* and *Phaeomegaceros sp. 2*). To consider the morphological variation, multiple accessions were included for *P. squamuliger* (3 samples), one of which is the subspecies *Phaeomegaceros squamuliger* subsp. *hasselii* Villarreal, Cargill & Goffinet (2010: 352), and *P. fimbriatus* (4 samples) one specimen represent a population from the Paramo habitats described by Villarreal and Renzaglia (2006). Paramos are ecosystems above the tree line (3000 m) at the top of the Andes from Ecuador, Colombia to Venezuela. Paramo habitats have contrasting temperatures during the day from 0° to 20°C, high relative humidity (>80%), and

precipitation ranging from 1000–4500 mm (Zapata *et al.* 2021). Two species of *Dendroceros* Nees (in Gottsche *et al.* 1846: 579), one species of *Megaceros* Campbell (1907: 484), and two species of *Nothoceros* (Schuster) Hasegawa (1994: 32) were used as the outgroup. We generated 52 new sequences from *Phaeomegaceros* and downloaded 58 sequences from GenBank (http://www.ncbi.nlm.nih.gov/genbank/), representing a total of fourteen morphological species in our molecular dataset. Species names, specimens examined, and GenBank accession numbers for all sequences are listed in Supplemental Table S1.

DNA extraction and sequence assembly—Genomic DNA was extracted from fresh and herbarium plant material using the NucleoSpin Plant II kit (Marcherey-Nagel, Düren, Germany) following the standard protocol with optional alcohol-based buffer (PW1) wash. Polymerase chain reactions (PCR) were used to amplify eight molecular markers: nuclear phytochrome (including two introns), mitochondrial *nad*5, and chloroplast markers of *rbcL*, *trnL* intron, *trnL-trnF* spacer, *rps4* gene, *rps4-trnS* spacer, and *matK* gene (Villarreal & Renner 2013, Villarreal & Renner 2014, Villarreal *et al.* 2015, Dawes *et al.* 2020).

Sequences were edited and aligned with Geneious 11.1.4 (https://www.geneious.com). Alignments were performed automatically using the default settings (65 % similarity, gap open penalty = 12, gap extension penalty = 3, refinement iterations = 2), and were checked manually. We tested the congruence among markers from the chloroplast, mitochondria, and nucleus separately using Maximum Likelihood (ML) approaches with the program RAxML-Blackbox and computing 1,000 bootstrap pseudoreplicates (Stamatakis 2006) under the Gamma model of rate heterogeneity. ML results indicated that the markers were not incongruent in the tree topology, even though the mitochondria and nuclear markers had little phylogenetic information. ML of the concatenated dataset showed a similar topology to the one observed with the separate markers (chloroplast specifically), but with greater resolution and statistical support for the genus *Phaeomegaceros* (Supplemental Figs. S1; S2; S3). We also measured the gene concordance factor and the site concordance factor in our dataset using IQ-TREE 2 (Minh *et al.* 2020). Concordance factors were calculated based on an inferred species tree with 1000 ultrafast bootstrap and an edge-linked partition model. Then, we inferred the gene tree for each of the eight markers to check for concordance among them (Supplemental Fig. S4). Gene concordance factors range between 20–66 %, indicating that at least two to five of the eight markers used to infer the phylogeny support the tree topology. Site concordance factors ranged between (18) 35–72 % of support for the tree topology observed. *Phaeomegaceros hirticalyx* (Stephani, 1916: 966) Duff, Villarreal, Cargill & Renzaglia (2007: 241) and *Phaeomegaceros coriaceus* (Stephani, 1916: 991) Duff, Villarreal, Cargill & Renzaglia (2007: 241) showed the lowest concordance factor, however, it did not affect the tree topology obtained from the different phylogenetic analyses. Since our dataset did not show major discordance among genes, a concatenated alignment was created with the eight loci resulting in a total of 6539 base pairs.

Phylogenetic analyses—Maximum parsimony (MP) analyses were carried out with PAUP* 4.0a146 (Swofford 2001). Maximum parsimony heuristic searches were conducted with the following parameters implemented: heuristic searches mode 100 random-addition-sequence replicates, tree bisection-reconnection (TBR) branch swapping, with multiple trees saved. All characters were treated as equally weighted and unordered. We evaluated the eight markers separately with the software PartitionFinder (Lanfear *et al.* 2016) to select the best-fit evolutionary model for each nucleotide marker. Separate alignments of the following markers were used in the software PartitionFinder: nuclear phytochrome, mitochondrial *nad*5, and chloroplast markers of *rbcL*, *trnL* intron, *trnL-trnF* spacer, *rps4* gene, *rps4-trnS* spacer, and *matK* gene. The evolutionary models were compared with exhaustive searches based on the Akaike Information Criterion (AIC) and the Bayesian information criterion. ML analyses were performed with the program RAxML-Blackbox computing 1000 bootstrap pseudoreplicates (Stamatakis 2006) under the Gamma model of rate heterogeneity. A 50% majority-rule consensus tree was computed from the 1000 bootstrapping pseudoreplicates with PAUP (Swofford 2001). Maximum parsimony and ML results were visualized in FigTree v1.4.3 (Rambaut 2014), and bootstrap values ≥ 70 were regarded as moderate and ≥ 85 as good support (Erixon *et al.* 2003).

Bayesian inference (BI) was performed on MrBayes v.3.2.6 (Ronquist & Huelsenbeck 2003, Ronquist *et al.* 2012) using the computational portal CIPRES Science Gateway (Miller *et al.* 2010). For the BI analysis, the models of evolution selected by PartitionFinder (Lanfear *et al.* 2016) were set for each separate marker (Supplemental Table S3). Default priors of model parameters were also defined for each partition. Two parallel Markov Chain Monte Carlo (MCMC) runs, each of 5 million generations, were conducted each run containing four chains with default priors on all the parameters. Trees and estimated parameter values were sampled every 1000 generations, thus obtaining a total of 10,000 samples from the combined runs, of which the first 10% of each (total 1000 trees) were discarded as burn-in. Burn-in and convergence of runs were verified using Tracer 1.6 (Rambaut *et al.* 2014). A majority-rule consensus tree was computed to calculate the Bayesian posterior probability (BPP), in which values of BPP ≥ 0.95 were considered significant.

Morphological assessment—Live collections and type specimens of the ten species, and one subspecies, of *Phaeomegaceros* were studied using light microscopy to describe the chloroplast morphology, thallus morphology, and antheridium number and size (Supplemental Table S2). Mature sporophytes were dissected, and spores were distributed on stubs covered with nail polish; these were coated with gold-palladium and examined with a FEG—Quanta 200 FEI Scanning Electron Microscope (SEM) housed at the Microscopy Center of the Federal University of Minas Gerais and at Southern Illinois University Carbondale.

Molecular clock dating—Sixteen accessions including nine species of *Phaeomegaceros* (Supplemental Table S1), and the outgroup were selected for the divergence times analyses. Two populations of *P. squamuliger* and *P. fimbriatus* were selected that exhibited varied morphological characters (Villarreal & Renzaglia 2006, Villarreal *et al.* 2010b). We used only the chloroplast markers (*rbcL*, *trnL* intron, *rps4* gene, *rps4-trnS* spacer, and *matK* gene) based on their variable parsimony-informative characters.

To evaluate the divergence time of the genus *Phaeomegaceros* we applied a fossil calibration based on the age of the fossil spores of *Phaeoceros* sp. *sensu* Graham (1987). This fossil is from the Uscari formation in Costa Rica that is dated around the Lower Miocene (15–23 Ma). The fossil has small spores (40–45 μm) with foveas in the distal face. The spores are nearly identical to those of the extant Neotropical species *Phaeomegaceros fimbriatus* which has six foveas in the distal face. Based on the previous phylogenetic reconstruction, the accessions of *P. fimbriatus* with this spore morphology cluster in one monophyletic clade (Fig. 1). A log-normal distribution on the prior (offset = 14.5, mean = 1, SD = 1; 95% interval = 15–28.6 Ma) was applied on the stem node of the clade containing *P. fimbriatus*. To improve the estimation accuracy of our analyses (Warnock *et al.* 2012), we applied a root constraint with a normal distribution (mean = 65 Ma, SD = 7.5) calibration at the node of divergence of the genus *Phaeomegaceros* within the family Dendrocerotaceae (Villarreal *et al.* 2015).

Divergence times were estimated using BEAST v1.8.4 (Drummond *et al.* 2012) with the previously mentioned substitution model with unlinked data partition for the five markers. The analysis was run separately with a pure-birth Yule tree prior and a Birth-Death tree prior. Each tree prior was run under a strict-clock and an uncorrelated log-normal relaxed clock model (Drummond *et al.* 2006). Tree prior and clock models were compared using Bayes factors based on path-sampling and stepping-stone sampling marginal likelihood estimates. Three independent runs of MCMC were run for 550 million generations with parameters sampled every 2500 generations. BEAST v1.8.4 was run using the CIPRES Science Gateway computational portal (Miller *et al.* 2010).

The convergence point was estimated by examining the three independent log files in Tracer 1.6 (Rambaut *et al.* 2014) to confirm that the separate analyses converged on the same point. Effective sampling size values > 200 were regarded as good sampling, indicating that the parameters had been sampled sufficiently for valid parameter estimation. After discarding the initial 10% of the trees as burn-in, a maximum clade credibility (MCC) tree with mean node heights was identified with TreeAnnotator 1.8.2 (part of the BEAST package). The results were visualized with Figtree v1.4.3 (Rambaut 2014). An additional analysis with an empty alignment was conducted to test the influence of the priors on posterior distributions. We report mean ages and 95% high posterior density (HPD) values.

Ancestral area reconstruction—We reconstructed the biogeography of *Phaeomegaceros* using BioGeoBEARS (Matzke 2014) in RASP v.4.2. (Yu *et al.* 2015). The distributional range of *Phaeomegaceros* was divided into five major areas: (A) New Zealand, (B) Southern-South America, (C) North, Central, and Northern-South America, (D) the Atlantic Island Tristan da Cunha, and (E) Antarctica. Species distributions were assigned based on literature and collection information. For the ancestral area reconstruction model, we relied on changes in dispersal probabilities in time and between areas, based on reconstructed geological events (Estrella *et al.* 2019). Here we assigned the probability of area connectivity on two-time slices: before 30 Ma and between 30–0 Ma (Supplemental Table S4), which we consider a higher probability of connectivity between Australasia and Austral America during the ice-free period in Antarctica allowing species colonization. We explored the role of Antarctica in shaping the transoceanic pacific disjunction in *Phaeomegaceros*, by considering it as a defined area for the ancestral reconstruction. Since there are no extant species or fossil records in Antarctica, we allow species with divergence times before 30 Ma to be present in Antarctica in that period. Because all the species of *Phaeomegaceros* have restricted distributions, the maximum number of areas was set at two.

The MCC tree generated in the divergence time analysis was used to infer the ancestral area probability. The models DEC (Ree & Smith 2008), DIVA (Ronquist 1997), and BayArea (Landis *et al.* 2013) and the parameter of founder event speciation estimated (*J*) used by BioGeoBEARS, were compared using likelihood values and the Akaike information criterion corrected for small sample sizes (AICc) (Matzke 2013; Matzke 2014).

Results

Phylogeny—From the concatenated alignments (6539 bp) of the 14 taxa in our molecular dataset, 5911 characters were constant (proportion =0.90), and 408 variable characters were parsimony-uninformative while 220 were parsimony-informative (Supplemental Table S3). MP, ML, and BI analyses show congruent tree topologies for all the principal clades which are summarized in Figure 1. The support values of each branch differed between the three phylogenetic analyses. Maximum parsimony and ML phylogenetic trees had better resolution of intraspecific and interspecific relationships, with low (>50) to good support (>75). BI analyses only present good support to the principal clades of *Phaeomegaceros* (BPP=>0.95).
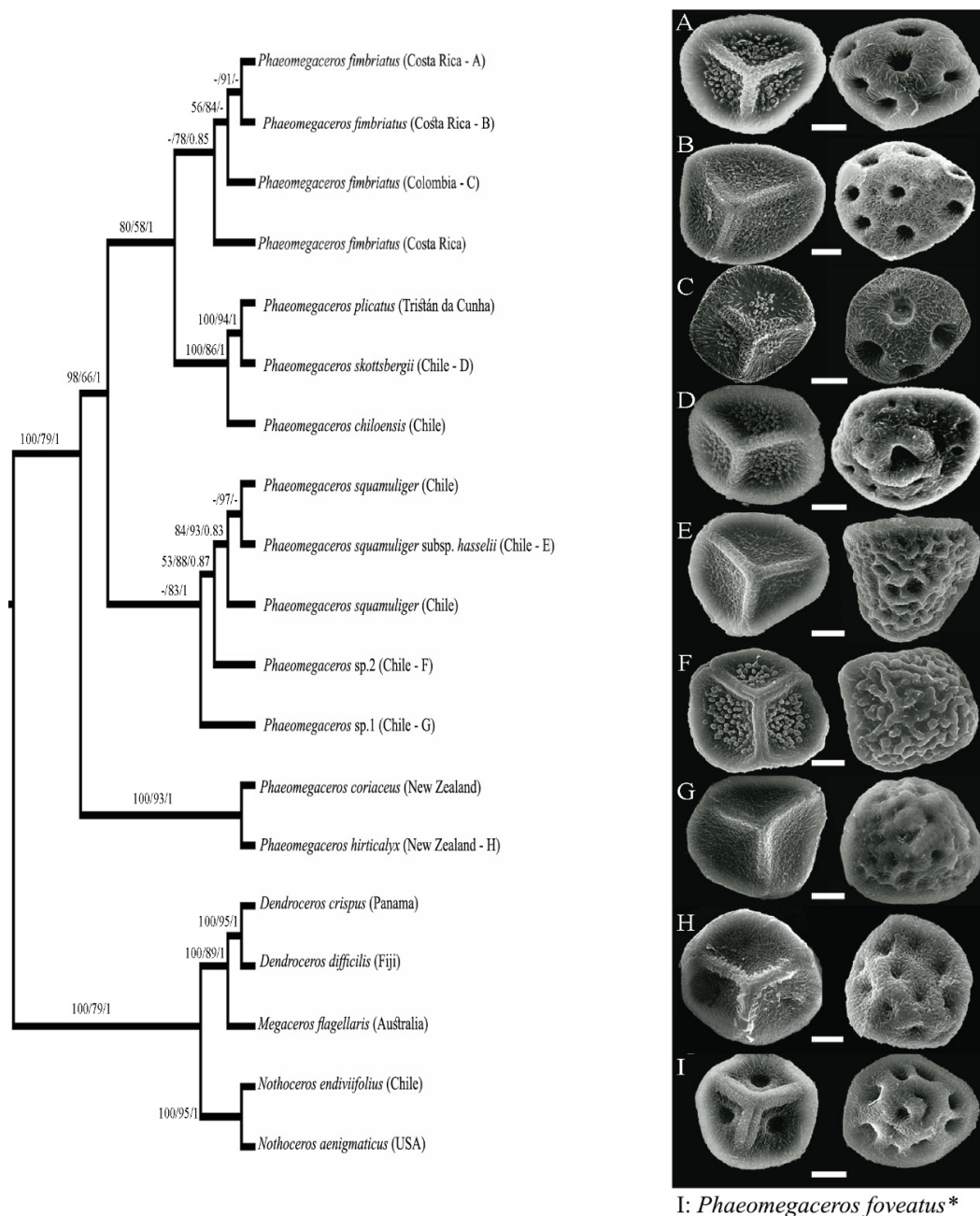

I: *Phaeomegaceros foveatus**

FIGURE 1. Majority-rule consensus phylogenetic tree of the genus *Phaeomegaceros* (Dendrocerotaceae) based on one nuclear, one mitochondrial and six chloroplast markers. Maximum parsimony values, ML bootstrap values and BPP values are depicted on branches, respectively. Bootstrap support values = <50 from one of the phylogenetic analyses are presented with a dash "-". Right column: SEM of proximal and distal spore faces from representative species on each clade. A, C: *Phaeomegaceros fimbriatus*; B: *Phaeomegaceros fimbriatus* collected in the Paramos; D: *Phaeomegaceros skottsbergii*; E: *Phaeomegaceros squamuliger* subsp. *hasselii*; F: *Phaeomegaceros* sp. 2; G: *Phaeomegaceros* sp. 1; H: *Phaeomegaceros hirticalyx*; I: *Phaeomegaceros foveatus** (not included in the phylogeny). Scale =10 μm.

Monophyly of *Phaeomegaceros* is strongly supported by all analyses (MP=100; ML=79.8; BPP=1.0). *Phaeomegaceros* is separated into two well-supported clades with contrasting geographic distributions. One clade is represented by the two New Zealand species *P. coriaceus* and *P. hirticalyx*, and the other clade includes species from the Americas and Tristan da Cunha (MP=100, ML=79, BPP=1.0). The American species are divided into three well-support clades (MP=98, ML=66, BPP=1.0). One clade comprises species from southern South America, including two undescribed species from Chile (*Phaeomegaceros sp. 1* and *Phaeomegaceros sp. 2*), sister to *P. squamuliger* (MP=53, ML=88, BPP=0.87) and *Phaeomegaceros squamuliger* subsp. *hasselii* (MP=84, ML=93, BPP=0.83). In the second clade *Phaeomegaceros chiloensis* (Stephani:1911; 90) Villarreal (2010b: 353) is resolved (MP=100, ML=86, BPP=1) as a sister to both island endemics: *Phaeomegaceros skottsbergii* (Stephani: 1911; 90) Duff, Villarreal, Cargill & Renzaglia (2007: 241) from Juan Fernández Island in the Southern Pacific Ocean, and *P. plicatus* from Tristan da Cunha, Southern Atlantic Ocean. The relationship between the latter two species has strong support in the three phylogenetic analyses (MP=100, ML=94, BPP=1). The third clade includes the two different morphotypes of *P. fimbriatus* distributed in Central and Northern-South America (ML=78, BPP=0.85).

Distinct spore architecture can serve as evidence that taxa belong to different morphospecies. Species of *Phaeomegaceros* from New Zealand have a trilete mark with a fovea on the spore proximal face, whereas Neotropical species lack foveas on the spore proximal face (Fig. 1; Campbell, 1993). Austral American species with low to strongly vermiculate or brain-like ornamentation on distal faces are resolved in one clade (*P. squamuliger*: Fig. 1E, *Phaeomegaceros sp. 1*: Fig. 1G, and *Phaeomegaceros sp. 2*: Fig. 1F). *Phaeomegaceros skottsbergii* (Fig.1D) has vermiculate spores with one large distal central fovea, surrounded by a protuberant ring and twelve shallow foveas (Fig. 1D). *Phaeomegaceros chiloensis* and *P. plicatus*, which are grouped with *P. skottsbergii,* present one distal central fovea (without a protuberant rim), surrounded by shallow foveas. *Phaeomegaceros fimbriatus* has a vermiculated distal face and well-marked foveas (four to seven) and a central fovea (Figs. 1A, 1B; Table 1). Populations of *P. fimbriatus* collected in the Paramos (above 3000 meters) when compared to the populations of *P. fimbriatus* from montane cloud forest, tend to present larger gametophytes (32 mm long, 3–4 mm wide), lack dorsal outgrowths, and with a long sporophyte (42 mm). The spores of samples from the Paramos tend to be larger (>45–61 µm), with the distal surface with more fovea 4–7(–9) fovea, and the proximal face with abundant vermiculae and coarse verrucae lacking (Figs. 1B, 3; Table 1; a detailed description of the morphological variation of *P. fimbriatus* collected in Paramos is provided in Supplemental File 1).
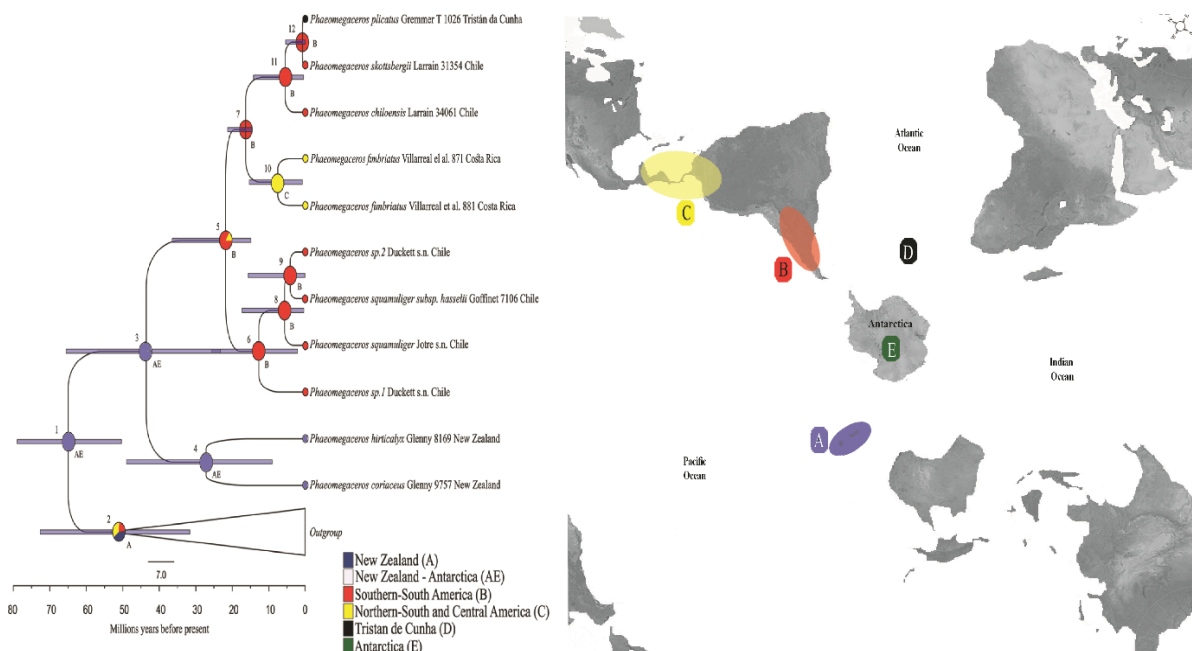

FIGURE 2. Divergence time chronogram of the genus *Phaeomegaceros* inferred from one mitochondrial and five chloroplast markers, under a relaxed clock model with fossil and root constraint calibration. Bars at nodes represent 95% HPD intervals around node ages. Pie charts at nodes represent probabilities for ancestral areas from BioGeoBEARS analysis with the BAYAREALIKE+J model. Color code circles represent sample distribution.

TABLE 2. Mean age divergence estimate in million years ago (Ma), 95% highest probability density intervals (HPD), and Bayesian posterior probability (BPP) of the clades of the genus *Phaeomegaceros* using a fossil calibration. The number in the clade column stands for the node age presented in Fig. 2. Bayesian posterior probability values ≥95 in bold. Log marginal likelihood for path sampling and stepping-stone test.

Node ID	Yule Strict clock		Yule relaxed clock		BD URC relaxed clock		BD strict clock	
	Age in Ma (HPD 95%)	BPP	Age in Ma (HPD 95%)	BPP	Age in Ma (HPD 95%)	BPP	Age in Ma (HPD 95%)	BPP
1	84.75 (73.24, 96.71)	**1**	64.96 (50.34, 78.97)	**1**	65.44 (51.23, 79.63)	**1**	84.92 (73.23, 96.72)	**1**
2	75.36 (63.33, 87.91)	**1**	53.51 (31.64, 72.63)	**1**	54.51 (33.16, 73.74)	**1**	75.5 (63.51, 88.17)	**1**
3	80.65 (68.41, 93.23)	**1**	43.57 (23.20, 65.52)	**1**	41.7 (21.84, 63.95)	**1**	80.84 (68.71, 93.49)	**1**
4	24.06 (18.80, 30.52)	**1**	27.17 (9.05, 48.98)	**1**	24 (7.73, 43.99)	**1**	24 (18.74, 30.40)	**1**
5	7 (4.11, 10.54)	**0.95**	21.82 (14.89, 36.47)	**1**	21.11 (14.87, 34.38)	**1**	15.1 (14.57, 16.09)	**1**
6	3.98 (2.02, 6.41)	**0.99**	12.74 (2.14, 25.69)	0.81	11.76 (1.86, 24.0)	0.84	3.87 (1.93, 6.23)	**0.99**
7	15.11 (14.57, 16.11)	**1**	16.33 (14.59, 21.26)	**0.97**	16.23 (14.58, 20.79)	**0.96**	6.87 (4.0, 10.34)	**0.95**
8	2.4 (0.85, 4.28)	0.52	5.65 (0.38, 17.29)	0.56	5.04 (0.35, 15.82)	0.57	2.32 (0.82, 4.16)	0.51
9	2.4 (0.68, 4.47)	0.52	4.14 (0.09, 15.62)	0.55	3.8 (0.13, 14.48)	0.54	2.32 (0.69, 4.4)	0.53
10	6.77 (3.58, 10.38)	**0.94**	7.51 (0.77, 15.37)	**1**	7.17 (0.72, 14.94)	**0.99**	6.68 (3.53, 10.25)	**0.94**
11	2.07 (0.63, 3.95)	**1**	5.51 (0.47, 14.15)	**1**	5.08 (0.43, 13.56)	**1**	2.02 (0.62, 3.86)	**1**
12	0.4 (0, 1.53)	**0.99**	0.76 (0, 5.34)	**0.99**	0.71 (0, 4.78)	**0.99**	0.38 (0, 1.47)	**0.99**
	Mean posterior	-9806.1		-9699.1		-9480.2		-9589.5
	Path sampling	-9463.1		-9278.8		-9278.7		-9463
	Stepping-stone	-9438.8		-9253.5		-9255.2		-9438.8

Divergence time and historical biogeography—An uncorrelated log-normal relaxed clock model was selected as the best clock model for our divergence times analyses. Birth-Death and Yule tree prior present similar results based on model comparison and similar divergence time estimates (Table 2). Divergence time and ancestral area reconstruction are summarized in Figure 2. The results indicated a New Zealand origin during the Late Cretaceous. When the Antarctic continent was included in the ancestral area reconstruction, a New Zealand-Antarctic origin is the most likely event (Supplemental Table S5). The probability of the origin in New Zealand-Antarctic (BPP. 0.83) is more likely than an origin from New Zealand alone (BPP. 0.39). Austral American species diverged around 43.57 Ma (HPD 95% = 23.20–65.52) during the Eocene (Fig. 2, Table 2), where both dispersal events and vicariance were reconstructed. The American species diverged during the Miocene (Table 2) from an Austral American ancestor (Supplemental Table S5). The biogeographical history model suggests that long-distance dispersal events to insular habitats (Oceanic islands and isolated mountains) is the main process driving the evolution of locally endemic species in the genus *Phaeomegaceros* (Table 3).

TABLE 3. BioGeoBEARS model comparisons based on log-likelihood (lnL) and the Akaike information criterion corrected for small sample sizes (AICc); *n*=number of parameters; *d*=rate of dispersal; *e*=rate of extinction; *j*=relative probability of founder-event speciation. The best model is shown in bold.

Without Antarctica	lnL	Number of parameters	*d*	*e*	*j*	AICc	AICc wt
DEC	-25.56	2	0.0079	1.00E-12	0	56.04	0.0003
DEC+J	-16.9	3	1.00E-12	1.00E-12	0.2	41.8	0.38
DIVALIKE	-22.14	2	0.0094	1.00E-12	0	49.2	0.0094
DIVALIKE+J	**-16.79**	**3**	**1.00E-12**	**1.00E-12**	**0.2**	**41.58**	**0.42**
BAYAREALIKE	-35.82	2	0.014	2.40E-02	0	76.56	1.10E-08
BAYAREALIKE+J	-17.61	3	1.00E-07	1.00E-07	0.18	43.22	0.19
Including Antarctica	lnL	Number of parameters	*d*	*e*	*j*	AICc	AICc wt
DEC	-31.25	2	0.013	1.00E-12	0	67.42	0.027
DEC+J	-28.18	3	0.0048	1.00E-12	0.15	64.37	0.12
DIVALIKE	-29.26	2	0.012	1.00E-12	0	63.44	0.19
DIVALIKE+J	-28.26	3	0.0077	1.00E-12	0.072	64.51	1.10E-01
BAYAREALIKE	-41.12	2	0.021	2.30E-02	0	87.16	1.40E-06
BAYAREALIKE+J	**-26.7**	**3**	**0.0016**	**1.00E-07**	**0.17**	**61.4**	**0.54**

Discussion

Taxonomic concepts around and within Phaeomegaceros—The four genera in the family Dendrocerotaceae have been evaluated using molecular markers and are geographically circumscribed as follows: *Megaceros* is restricted to Asia and Australasia, *Nothoceros* occurs in New Zealand and the Americas, *Dendroceros* is widespread in the Neotropics and Australasia, and *Phaeomegaceros* is distributed in Australasia, Austral and Central America, and Tristan da Cunha (Villarreal *et al.* 2010a, Villarreal *et al.* 2010c, Villarreal & Renner 2014, Villarreal *et al.* 2015). Duff *et al.* (2007) established *Phaeomegaceros* based on a set of clear-cut morphological features. A previous large-scale hornwort phylogeny failed to resolve it as a well-supported monophyletic genus (Villarreal *et al.* 2010b, Villarreal & Renner 2013). Here, by analyzing almost all species (9/10 spp.) with eight molecular markers, the genus *Phaeomegaceros* is strongly supported. Furthermore, the synapomorphies of *Phaeomegaceros* described by Duff *et al.* (2007), such as a single antheridium per chamber, the lack of a pyrenoid and possession of stomata are supported. The presence of the foveolate and vermiculate spores represents a diagnostic character for most of the *Phaeomegaceros* species (except for *Phaeomegaceros sp. 2* with a brain-like ornamentation on the spore distal face). *Phaeomegaceros foveatus* (Hasegawa, 2001; 374) Villarreal (2010b: 352) and a Javanese population identified as *P. hirticalyx* (Hasegawa 1988, Campbell & Hasegawa 1993) were not included in the present phylogeny due to the lack of material for sequencing. Based on morphology we expect these species to be closely related to the New Zealand clade.

Our phylogeny recovers two well-supported clades, one with the New Zealand taxa, and another with the American taxa (including one Atlantic Ocean species). *Phaeomegaceros plicatus*, *P. chiloensis,* and *P. skottsbergii* cluster in a monophyletic group with good support. The phylogenetic relationships of *P. squamuliger* and the two undescribed species from Chile needs further investigation since they are only supported by the MP analysis. However, both undescribed taxa from Chilean collections have distinctive spore and gametophyte morphology (Table 1, Fig. 1, Jeff Duckett, *pers. comm.*).

Phaeomegaceros fimbriatus is commonly found in medium to high-altitude tropical forests, and its distribution ranges from Northern South America to North America (Mexico), with a wide variation in gametophyte and spore morphology (Villarreal & Renzaglia 2006; Ibarra-Morales *et al.* 2020). The species is diagnosed by a distal face with a central fovea surrounded by four to seven foveas. Fossilized spores with the diagnostic distal foveas were found abundantly in the Miocene Uscari formation in Costa Rica (Graham 1987), identifying the distribution of this species throughout the Neotropics since 15–23 Ma.

All accessions of *P. fimbriatus* are grouped in a single clade, despite differences in the size of the thallus, spore size, and the distinct spore proximal face ornamentation in the two morphotypes respectively found in montane cloud

forests (700–2000 m) and Paramo populations above 3200 m (Villarreal and Renzaglia 2006; Hasegawa 2001). Paramo populations of *P. fimbriatus* differ from the populations in lower altitudes by their more robust sporophytes (9–13 assimilative cells vs. 6–9 in lower altitudes), the smooth surface of the gametophyte (including involucre), thicker thallus and larger spores (45–61 mm vs. 32–43 mm in diameter). The spore ornamentation of *P. fimbriatus* and allied species such as *P. skottsbergii* are characterized by a pronounced central fovea surrounded by various numbers of foveas (Fig. 3, Hässel de Menéndez 1989; Hasegawa 2001). The proximal face of the spores has coarse verrucae in *P. fimbriatus* (Hässel de Menéndez 1989; Hasegawa 2001; Villarreal & Renzaglia 2006). Based on the stomatal size, spore size, and overall exuberant growth, Villarreal and Renzaglia (2006) speculated on a possible autopolyploidy origin of this taxon. Polyploidy in hornworts has been rarely documented and warrants further research (Proskauer 1957; Newton 1983). Our analysis using eight molecular markers resolved all accessions of *P. fimbriatus* in a polytomy or with low support, including the accession of *P. fimbriatus* from Paramo. This result indicated that despite Paramo plants being morphologically distinct, the markers used in the present dataset are not suitable for resolving the intraspecific relationships among these individuals in *Phaeomegaceros* (Villarreal *et al.* 2015).
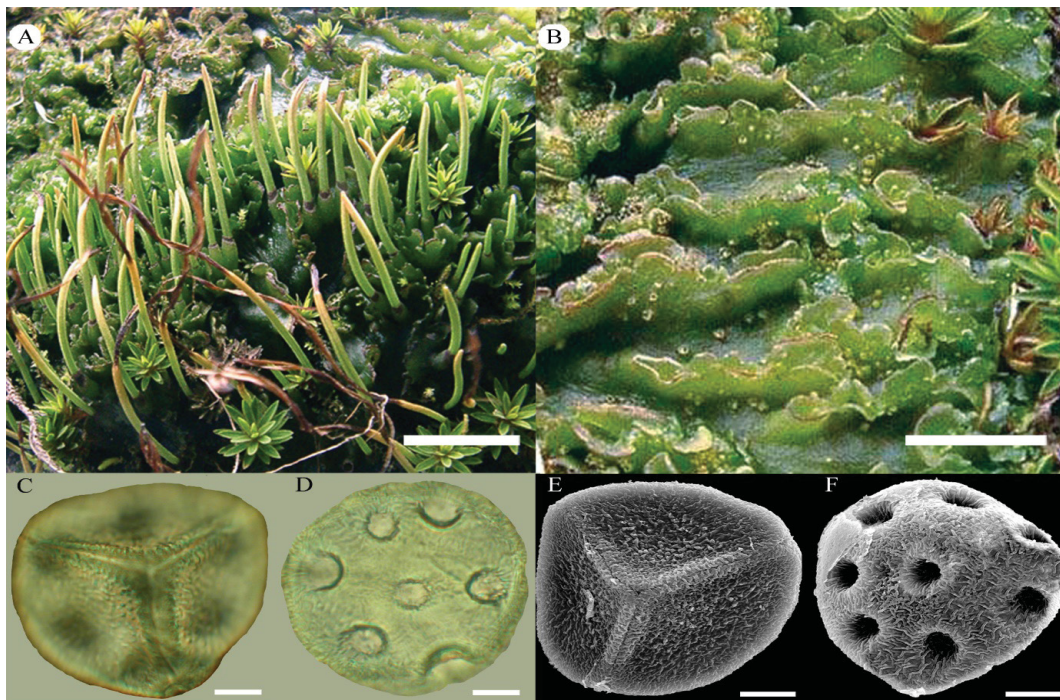

FIGURE 3. Populations of *P. fimbriatus* collected in the Páramos. A: Female plant habit with sporophytes; B: Male plant habit; C: Proximal spore side; D: Distal spore side; E: SEM Proximal spore side; D: SEM Distal spore side. Scale: A = 10 mm; B = 5 mm; C-F = 10 μm.

Austral biogeography and allopatric speciation in *Phaeomegaceros*—Our estimates showed that *Phaeomegaceros* diverged from other Dendrocerotaceae genera between 50–79 Ma from a New Zealand /Antarctica ancestor. The present estimates correspond to the Late Cretaceous diversification of most extant species of hornworts (Laenen *et al.* 2014; Villarreal *et al.* 2015). The American lineage diverged from New Zealand, between ~21–65 Ma in the Paleogene. The beginning of the Gondwanan continental break-up is estimated around 82 Ma. Our estimates suggest a long-distance oceanic dispersal scenario from New Zealand to Austral America during this period as a more plausible explanation (de Queiroz 2005). Oceans may only act as barriers between continents when air currents are not conducive to dispersal of spores (Muñoz *et al.* 2004, De Queiroz 2005, Vanderpoorten *et al.* 2008). Eastward long-distance dispersal event from New Zealand to Austral America could lead to the transoceanic connectivity between both regions (Sanmartín *et al.* 2007). Moreover, the capacity of bryophytes for long-distance dispersal is consistent with an explanation of a transoceanic disjunction in the Pacific Ocean through dispersal events (Heinrichs *et al.* 2009; McDaniel & Shaw 2003; Villarreal & Renner 2014; Carter *et al.* 2017). In ferns, however, both dispersal events and vicariance shaped current distribution patterns between Australasia and Austral America (Morero *et al.* 2019, Korall & Pryer 2014).

Australasia/southern South America has experienced changes in wind currents and climatic fluctuations through geological times (Lewis *et al.* 2008; Mao *et al.* 2012; Sanmartín *et al.* 2007; Sérsic *et al.* 2011; Quiroga & Premoli 2010). From the Early Paleogene to Late Pleistocene, the Antarctic continent's climate varied from warm and wet to

very cold and dry savannas (Ortiz-Jaureguizar & Caldera 2006). Bryophyte species might have occupied this area maintaining contact between New Zealand and Austral America (Carter *et al.* 2017; Sun *et al.* 2014), through stepping-stone dispersal among suitable vegetation, even in periods of recent glaciations in Antarctica during the Eocene (Truswell & Macphail 2009; Pisa *et al.* 2014). When Antarctica was not included as a state area in the analysis, New Zealand was reconstructed as a possible origin for the genus. When Antarctica was included in the analyses as a main area in the ancestral area reconstruction (Estrella *et al.* 2019), a New Zealand-Antarctic origin, with both dispersal events and vicariance reconstructed for the origin of Austral America taxa. Based on our most plausible hypothesis, hornworts may have occupied Antarctica during the Eocene and later went extinct with the advancement of glaciation as suggested for other organisms, including bryophytes (Lewis *et al.* 2008). Nevertheless, Antarctica as a biome may have played a large role in the current distribution of Austral disjunct lineages, allowing contact between New Zealand and Southern South America during the Cretaceous and Early Cenozoic (Estrella *et al.* 2019; Macphail *et al.* 2022).

The diversification of *Phaeomegaceros* in Austral America could be related to dispersal and further cladogenesis (regional allopatric processes occurring in insular habitats, such as mountains or islands: sensu Emerson & Patiño 2018). In South America during the Miocene, climatic and habitat changes along the continent occurred with the mountain uplift along the Andes cordillera (Hoorn *et al.* 2010). The Southern Andes experienced an uplift of >1000 m between ~22 to 14 Ma (Ortiz-Jaureguizar & Cladera 2006), and with the final development of the Paramos in the last 3–5 million years, changing local climate from dry to humid rainforests in northern South America (Parrish 1989). These conditions have been shown to favor bryophyte northward expansion from Austral America (McDaniel & Shaw 2003; Villarreal & Renner 2014) to mountain forests in tropical America. Our results support this cladogenic scenario with the divergences of *Phaeomegaceros* species tracking the origin of suitable conditions along the Andes cordillera. To our knowledge, this represents the first attempt to relate regional orogenic process with hornwort evolution; and add evidence of landscape changes driving the species diversification as climate conditions change and new habitats become available.

The divergence of the two island endemic species, *P. skottsbergii* and *P. plicatus*, suggests cladogenic speciation to oceanic islands (Emerson & Patiño 2018). Our divergence time estimates of *P. plicatus*, endemic to Tristan da Cunha, and *P. skottsbergii,* endemic to Juan Fernandez, correspond to both volcanic island formation periods around ~1 Ma (Gass 1967) and 1–4 Ma (Stuessy *et al.* 1984), respectively. Both species are nested with *P. chiloensis*, which is found more than ~700 km from Juan Fernandez and more than ~4500 km from Tristan da Cunha Island. Cryptogam island endemic taxa are a common example of long-distance dispersal and cladogenic processes (Patiño *et al.* 2014) and were observed in the hornwort *Anthoceros cristatus* on Ascension Island from a European ancestor (Villarreal *et al.* 2017).

In conclusion, we present a phylogenetic reconstruction of the genus *Phaeomegaceros* and described the distinct spore morphologies that support species delimitation (Villarreal *et al.* 2010a). In addition, we show that the historical biogeography of the genus points to the role of the Antarctic continent as a major biogeographical area that shaped the current disjunct distribution between Australasia and Austral America (Estrella *et al.* 2019; Macphail *et al.* 2022). Finally, long-distance dispersal and cladogenesis processes drove the colonization of the two distinct *Phaeomegaceros* species on the oceanic islands of Juan Fernandez and Tristan da Cunha.

Author contributions

JCVA conceived the study. JCVA and GFPB conducted fieldwork, herbarium study, and taxonomic descriptions. AMS, GFPB, HB and JCVA did the laboratory work. AMS processed and analyzed the data. All authors contributed to the writing of the manuscript.

References

Biersma, E.M., Jackson, J.A., Stech, M., Griffiths, H., Linse, K., & Convey, P. (2018) Molecular data suggest long-term in situ Antarctic persistence within Antarctica's most speciose plant genus, *Schistidium*. *Frontiers in Ecology and Evolution* 6: 77.
https://doi.org/10.3389/fevo.2018.00077

Blöcher, R. & Frahm, J.-P. (2002) A comparison of the moss floras of Chile and New Zealand. Studies in austral temperate rain forest bryophytes 17. *Tropical Bryology* 21: 81–92.
https://doi.org/10.11646/bde.21.1.13

Blume, C.I. (1850) Lugduno-Batavum, sive, Stirpium exoticarum novarum vel minus cognitarum ex vivis aut siccis brevis expositio et descriptio. *Museum botanicum* 1: 307.Campbell, D. 1907. Studies on some Javanese Anthocerotaceae. I. *Annals of Botany* 21: 467–486.
https://doi.org/10.5962/bhl.title.274

Campbell, E.O. & Hasegawa, J. (1993). *Phaeoceros hirticalyx* (Steph.) Haseg. (Anthocerotae) new to New Zealand. *New Zealand Journal of Botany* 31: 127–131.
https://doi.org/10.1080/0028825X.1993.10419488

Campbell, D. (1907) Studies on Some Javanese Anthocerotaceae. *Annals of Botany*, 21, 467–486.
https://doi.org/10.1093/oxfordjournals.aob.a089148

Carter B.E., Larraín, J., Manukjanová, A., Shaw, B., Shaw, A.J., Heinrichs, J., de Lange, P., Suleiman, M., Thouvenot, L., & von Konrat, M. (2017) Species delimitation and biogeography of a southern hemisphere liverwort clade, *Frullania* subgenus *Microfrullania* (Frullaniaceae, Marchantiophyta). *Molecular Phylogenetics and Evolution* 107: 16–26.
https://doi.org/10.1016/j.ympev.2016.10.002

Dawes, T.N., Villarreal, J.C., Szövényi, P., Bisang, I., Li, F.-W., Hauser, D.A., Quandt, D., Cargill, D.C., & Forrest, L.L. (2020) Extremely low genetic diversity in the European clade of the model bryophyte *Anthoceros agrestis*. *Plant Systematics and Evolution* 306: 49.
https://doi.org/10.1007/s00606-020-01676-6

de Queiroz, A. (2005) The resurrection of oceanic dispersal in historical biogeography. *Trends in Ecology and Evolution* 20: 68–73.
https://doi.org/10.1016/j.tree.2004.11.006

Duff, R.J., Villarreal, J.C., Cargill, D.C., & Renzaglia, K.S. (2007) Progress and challenges in hornwort phylogenetic reconstruction. *The Bryologist* 110: 214–243.
https://doi.org/10.1639/0007-2745(2007)110[214:PACTDA]2.0.CO;2

Drummond, A.J., Ho, S.Y., Phillips, M.J., & Rambaut, A. (2006) Relaxed phylogenetics and dating with confidence. *PLoS Biology* 4, e88.
https://doi.org/10.1371/journal.pbio.0040088

Drummond, A.J., Suchard, M.A., Xie, D., & Rambaut, A. (2012) Bayesian phylogenetics with BEAUti and the BEAST 1.7. *Molecular Biology and Evolution* 29: 1969–1973.
https://doi.org/10.1093/molbev/mss075

Emerson, B.C. & Patiño, J. (2018) Anagenesis, Cladogenesis, and Speciation on Islands. *Trends in Ecology and Evolution* 33: 488–491.
https://doi.org/10.1016/j.tree.2018.04.006

Erixon, P., Svennblad, B., Britton, T. & Oxelman, B. (2003) Reliability of Bayesian posterior probabilities and bootstrap frequencies in phylogenetics. *Systematic Biology* 52: 665–673.
https://doi.org/10.1080/10635150390235485

Estrella, M., Buerki, S., Vasconcelos, T., Lucas, E.J., & Forest, F. (2019) The role of Antarctica in biogeographic reconstruction: A point of view. *International Journal of Plant Science* 180: 63–71.
https://doi.org/10.1086/700581

Frey, W., Stech, M., & Meißner, K. (1999) Chloroplast DNA-relationship in palaeoaustral *Lopidium concinnum* (Hypopterygiaceae, Musci). An example of steno-evolution in mosses. Studies in austral temperate rain forest bryophytes 2. *Plant Systematics and Evolution* 218: 67–75.
https://doi.org/10.1007/BF01087035

Gass, I. (1967) Geochronology of the Tristan da Cunha Group of Islands. *Geological Magazine* 104: 160–170.
https://doi.org/10.1017/S0016756800040620

Gasson, E.G.W. & Keisling, B.A. (2020) The Antarctic Ice Sheet: A Paleoclimate Modeling Perspective. *Oceanography* 33: 90–100.
https://doi.org/10.5670/oceanog.2020.208

Graham, A. (1987) Miocene Communities and Paleoenvironments of Southern Costa Rica. *American Journal of Botany* 74: 1501–1518.
https://doi.org/10.1002/j.1537-2197.1987.tb12142.x

Gottsche, C., Lindenberg, J. & Nees, C. (1846). *Synopsis hepaticarum*, fasc. 4. Meissner, Hamburg, 465–624.

Gottsche, C.M. (1964). Hepaticae, in: Triana, J., Planchon, J.. (Eds.), Prodromus Florae Novo-Granatensis Ou Énumeration Des Plantes de La Nouvelle-Grenade Avec Description Des Espèces Nouvelles. Annales des sciences naturelles, *Botanique*, 95–198.

Hasegawa, J. (1988) A proposal for a new system of the Anthocerotae, with a revision of the genera. *Journal of the Hattori Botanical Laboratory* 74: 105–119.

Hasegawa, J. (1994) New classification of Anthocerotae. *Journal of the Hattori Botanical Laboratory* 76: 21–34.

Hasegawa, J. (2001) A new species of *Phaeoceros* with remarkable spore features from Southeast Asia. *Bryological Research* 7: 373–377.

Hässel de Menéndez, G.G. (1989) Las especies de *Phaeoceros* (Anthocerotophyta) de América del Norte, Sud y Central; la ornamentación de sus esporas y taxonomía. *Candollea* 44: 715–739.

Heinrichs, J., Hentschel, J., Feldberg, K., Bombosch, A., & Schneider, H. (2009) Phylogenetic biogeography and taxonomy of disjunctly distributed bryophytes. *Journal of Systematics and Evolution* 47: 497–508.
https://doi.org/10.1111/j.1759-6831.2009.00028.x

Hill, R.S. (2001) Biogeography, evolution and palaeoecology of *Nothofagus* (Nothofagaceae): the contribution of the fossil record. *Australian Journal of Botany* 49: 321–332.
https://doi.org/10.1071/BT00026

Hoorn, C., Wesselingh, F.P., ter Steege, H., Bermúdez, M.A., Mora, A., Sevink, J., Sanmartín, I., Sanchez-Meseguer, A., Anderson, C.L., Figueiredo, J.P., Jaramillo, C., Riff, D.D., Negri, F.R., Hooghiemstra, H., Lundberg, J., Stadler, T., Särkinen, T., & Antonelli, A. (2010) Amazonia through time: Andean uplift, climate change, landscape evolution and biodiversity. *Science* 330: 927–931.
https://doi.org/10.1126/science.1194585

Ibarra-Morales A., Valencia-Avalos, S., & Muñiz-Díaz De León, M.E. (2020) Anatomy and Morphology of *Phaeomegaceros fimbriatus* (Gottsche) R.J.Duff, J.C.Villarreal, Cargill & Renzaglia (Anthocerotophyta), a Novel Record for North America. *Cryptogamie, Bryologie* 41: 219–228.
https://doi.org/10.5252/cryptogamie-bryologie2020v41a17

Knapp, M., Stöckler, K., Havell, D., Delsuc, F. Sebastiani, F., & Lockhart, P.J. (2005) Relaxed molecular clock provides evidence for long-distance dispersal of *Nothofagus* (southern beech*). PLoS Biol*. 3: e14.
https://doi.org/10.1371/journal.pbio.0030014

Korall, P. & Pryer, K.M. (2014) Global biogeography of scaly tree ferns (Cyatheaceae): Evidence for Gondwanan vicariance and limited transoceanic dispersal. *Journal of Biogeography* 41: 402–413.
https://doi.org/10.1111/jbi.12222

Laenen, B., Shaw, B., Schneider, H., Goffinet, B., Paradis, E., Désamoré, A., Heinrichs, J., Villarreal, J.C., Gradstein, S.R., McDaniel, S.F., Long, D.G., Forrest, L.L., Hollingsworth, M.L., Crandall-Stotler, B., Davis, E.C., Engel, J., von Konrat, M., Cooper, E.D., Patiño, J., Cox, C.J., Vanderpoorten, A. & Shaw, A.J. (2014) Extant diversity of bryophytes emerged from successive post-Mesozoic diversification bursts. *Nature Communications* 5: 5134.
https://doi.org/10.1038/ncomms6134

Landis, M.J., Matzke, N.J., Moore, B.R., & Huelsenbeck, J.P. (2013) Bayesian analysis of biogeography when the number of areas is large. *Systematic Biology* 62: 789–804.
https://doi.org/10.1093/sysbio/syt040

Lanfear, R., Frandsen, P.B., Wright, A.M., Senfeld, T. & Calcott, B. (2016) PartitionFinder 2: New Methods for Selecting Partitioned Models of Evolution for Molecular and Morphological Phylogenetic Analyses. *Molecular Biology and Evolution* 34: 772–773.
https://doi.org/10.1093/molbev/msw260

Lewis, A.R., Marchant, D.R., Ashworth, A.C., Hedenäs, L., Hemming, S.R., Johnson, J.V., Leng, M.J., Machlus, M.L., Newton, A.E., Ian Raine, J., Willenbring, J.K., Williams, M., & Wolfe, A.P. (2008) Mid-Miocene cooling and the extinction of tundra in continental Antarctica. *Proceedings of the National Academy of Sciences U.S.A.* 105: 10676–10680.
https://doi.org/10.1073/pnas.0802501105

Linder, H.P. & Crisp, M.D. (1995) *Nothofagus* and pacific biogeography. *Cladistics* 11: 5–32.
https://doi.org/10.1111/j.1096-0031.1995.tb00002.x

Macphail, M., Carpenter, R., & Hill, R. (2022) Formal recognition of extinct Antarctic polar forests as a distinct biome. *Antarctic Science, 34*(4): 343–347.
https://doi.org/10.1017/S0954102022000190

Mao, K., Milne, R.I., Zhang, L., Peng, Y., Liu, J., Thomas, P., Mill, R.R., & Renner, S.S. (2012) Distribution of living Cupressaceae reflects the breakup of Pangea. *Proceedings of the National Academy of Sciences U.S.A.* 109: 7793–7798.
https://doi.org/10.1073/pnas.1114319109

Markgraf, V., McGlone, M. & Hope, G. (1995) Neogene paleoenvironmental and paleoclimatic change in southern temperate ecosystems:

a southern perspective. *Trends in Ecology and Evolution* 10: 143–147.

https://doi.org/10.1016/S0169-5347(00)89023-0

Matzke, N.J. (2013) Probabilistic historical biogeography: New models for founder-event speciation, imperfect detection, and fossils allow improved accuracy and model-testing. *Frontiers of Biogeography* 5: 242–248.

https://doi.org/10.21425/F5FBG19694

Matzke, N.J. (2014) Model selection in historical biogeography reveals that founder-events Speciation is a crucial process in island clades. *Systematic Biology* 63: 951–970.

https://doi.org/10.1093/sysbio/syu056

McDaniel, S.F. & Shaw, A.J. (2003) Phylogeographic structure and cryptic speciation in the trans–Antarctic moss *Pyrrhobryum mnioides*. *Evolution* 57: 205–215.

https://doi.org/10.1111/j.0014-3820.2003.tb00256.x

Meißner, K., Frahm, J.-P., Stech, M. & Frey, W. (1998) Molecular divergence patterns and infrageneric relationship of *Monoclea* (Monocleales, Hepaticae). Studies in austral temperate rain forest bryophytes 1. *Nova Hedwigia* 67: 289–302.

https://doi.org/10.1127/nova.hedwigia/67/1998/289

Miller, M.A., Pfeiffer, W. & Schwartz, T. (2010) Creating the CIPRES Science Gateway for inference of large phylogenetic trees" in Proceedings of the Gateway Computing Environments Workshop (GCE).

https://doi.org/10.1145/2335755.2335836

Minh, B. Q., Hahn, M.W. & Lanfear, R. (2020) New methods to calculate concordance factors for phylogenomic datasets. *Molecular Biology and Evolution* 37: 2727–2733.

https://doi.org/10.1093/molbev/msaa106

Mitten, W. (1868) List of Samoan mosses in Journal of the Linnean Society. *Botany* 10: 174–175.

https://doi.org/10.1111/j.1095-8339.1868.tb02029.x

Mitten, W. (1884). Hepaticae, in: Report on the Scientific Results of the Voyage of H.M.S. Challenger during the Years 1873-76 : *Under the Command of Captain George S. Nares, R.N., F.R.S. and Captain Frank Turle Thomson, R.N./ Prepared under the Superintendence of Sir C.* Wyville Thomson. Publisher by Order of the Maiesty's Gobernment, Edinburgh, 176–178.

https://doi.org/10.5962/bhl.title.6513

Morero R.E., Deanna, R., Barboza, G.E. & Barrington, D.S. (2019) Historical biogeography of the fern genus *Polystichum* (Dryopteridaceae) in Austral South America. *Molecular Phylogenetics and Evolution* 137: 168–189.

https://doi.org/10.1016/j.ympev.2019.05.004

Muñoz, J., Felicísimo, Á.M., Cabezas, F., Burgaz, A.R. & Martínez, I. (2004) Wind as a long-distance dispersal vehicle in the Southern Hemisphere. *Science* 304: 1144–1147.

https://doi.org/10.1126/science.1095210

Newton, M. (1983) Cytology of the Hepaticae and Anthocerotae, Pp. 117–148 in *New Manual of Bryology*, vol. 1., ed. R. M. Schuster. Hattori Botanical Laboratory, Nichinan, Japan.

Ortiz-Jaureguizar, E. & Cladera, G.A. (2006) Paleoenvironmental evolution of southern South America during the Cenozoic. *Journal of Arid Environments* 66: 498–532.

https://doi.org/10.1016/j.jaridenv.2006.01.007

Parrish, J.T. (1989) Gondwanan paleogeography and paleoclimatology, Pp. 15–26 in *Antarctic paleobiology: its role in the reconstruction of Gondwana*, eds. T. N. Taylor and E. L. Taylor. Springer-Verlag, New York.

https://doi.org/10.1007/978-1-4612-3238-4_2

Patiño, J., Carine, M., Fernández-Palacios, J.M., Otto, R., Schaefer, H. & Vanderpoorten, A. (2014) The anagenetic world of spore-producing land plants. *New Phytologist* 201: 305–311.

https://doi.org/10.1111/nph.12480

Pfeiffer, T. (2000) Relationship and divergence patterns in *Hypopterygium* 'rotulatum' s.l. (Hypopterygiaceae, Bryopsida) inferred from *trnL* intron sequences. Studies in austral temperate rain forest bryophytes 7. *Edinburgh Journal of Botany* 57: 291–307.

https://doi.org/10.1017/S0960428600000226

Pisa, S., Biersma, E.M., Convey, P., Patiño, J., Vanderpoorten, A., Werner, O., & Ros, R.M. (2014) The cosmopolitan moss *Bryum argenteum* in Antarctica: recent colonisation or in situ survival? *Polar Biology* 37: 1469–1477.

https://doi.org/10.1007/s00300-014-1537-3

Pokorny, L., Oliván, G. & Shaw, A.J. (2011) Phylogeographic Patterns in Two Southern Hemisphere Species of *Calyptrochaeta* (Daltoniaceae, Bryophyta). *Systematic Botany* 36: 542–553.

https://doi.org/10.1600/036364411X583529

Proskauer, J. (1957) Anthocerotales, Pp. 19 in *Hepaticae from Juan Fernández Islands*, ed. S. W. Arnell. Arkiv für Botanik 4.

Pross, J., Contreras, L., Bijl, P., Greenwood, D.R., Bohaty, S.M., Schouten, S., Bendle, J.A., Röhl, U., Tauxe, L., Raine, J.I., Huck, C.E.,

van de Flierdt, T., Jamieson, S.S.R., Stickley, C.E., van de Schootbrugge, B., Escutia, C., Brinkhuis, H. & Integrated Ocean Drilling Program Expedition 318 Scientists. (2012) Persistent near-tropical warmth on the Antarctic continent during the early Eocene epoch. *Nature* 488: 73–77.
https://doi.org/10.1038/nature11300

Quandt, D., Frey, W. & Frahm, J.-P. (2001) Patterns of molecular divergence within the palaeoaustral genus *Weymouthia* Broth. (Lembophyllaceae, Bryopsida). Studies in austral temperate rainforest bryophytes 11. *Journal of Bryology* 23: 305–311.
https://doi.org/10.1179/jbr.2001.23.4.305

Quiroga, M.P. & Premoli, A.C. (2010) Genetic structure of *Podocarpus nubigena* (Podocarpaceae) provides evidence of Quaternary and ancient historical events. *Palaeogeography, Palaeoclimatology, Palaeoecology* 285: 186–193.
https://doi.org/10.1016/j.palaeo.2009.11.010

Rambaut, A. (2014) FigTree v1.4.2. Available from. http://tree.bio.ed.ac.uk/software/figtree/

Rambaut, A., Suchard, M.A., Xie, W. & Drummond, A.J. (2014) TRACER v.1.6, Available from. http://tree.bio.ed.ac.uk/software/tracer.

Renner, S.S., Foreman, D.B. & Murray, D. (2000) Timing transantarctic disjunctions in the Atherospermataceae (Laurales): evidence from coding and noncoding chloroplast sequences. *Systematic Biology* 49: 579–591.
https://doi.org/10.1080/10635159950127402

Roads, E., Longton, R. E. & Convey, P. (2014) Millennial timescale regeneration in a moss from Antarctica. *Current Biology* 24: 222–223.
https://doi.org/10.1016/j.cub.2014.01.053

Ronquist, F. (1997) Dispersal-vicariance analysis: a new approach to the quantification of historical biogeography. *Systematic Biology* 46: 195–203.
https://doi.org/10.1093/sysbio/46.1.195

Ronquist, F. & Huelsenbeck, J. P. (2003) MrBayes3: Bayesian phylogenetic inference undermixed models. *Bioinformatics* 19: 1572–1574.
https://doi.org/10.1093/bioinformatics/btg180

Ronquist, F., Teslenko, M., Van der Mark, P., Ayres, D. L., Darling, A., Höhna, S., Larget, B., Liu, L., Suchard, M.A. & Huelsenbeck, J.P. (2012) MrBayes 3.2: efficient Bayesian phylogenetic inference and model choice across a large model space. *Systematic Biology* 61: 539–542.
https://doi.org/10.1093/sysbio/sys029

Sanmartín, I. & Ronquist, F. (2004) Southern Hemisphere biogeography inferred by event-based models: plant versus animal patterns. *Systematic Biology* 53: 216–243.
https://doi.org/10.1080/10635150490423430

Sanmartín, I., Wanntorp, L. & Winkworth, R.C. (2007) West Wind Drift revisited: testing for directional dispersal in the Southern Hemisphere using event-based tree fitting. *Journal of Biogeography* 34: 398–416.
https://doi.org/10.1111/j.1365-2699.2006.01655.x

Sauquet, H., Ho, S.Y., Gandolfo, M.A., Jordan, G.J., Wilf, P., Cantrill, D.J., Bayly, M.J., Bromham, L., Brown, G.K., Carpenter R.J., Lee, D.M., Murphy, D.J., Sniderman J.M.K. & Udovicic, F. (2012) Testing the impact of calibration on molecular divergence times using a fossil-rich group: the case of Nothofagus (Fagales). Systematic Biology 61: 289–313.
https://doi.org/10.1093/sysbio/syr116

Schofield, W. & Crum, H. (1972) Disjunctions in bryophytes. *Annals of the Missouri Botanical Garden* 59: 174–202.
https://doi.org/10.2307/2394752

Setoguchi, H., Ono, M., Doi, Y., Koyama, H. & Tsuda, M. (1997) Molecular phylogeny of *Nothofagus* (Nothofagaceae) based on the *atpB-rbcL* intergenic spacer of the chloroplast DNA. *Journal of Plant Research* 110: 469–484.
https://doi.org/10.1007/BF02506808

Sérsic, A.N., Cosacov, A., Cocucci, A.A., Johnson, L.A., Pozner, R., Avila, L.J., Sites Jr., J.W. & Morando, M. (2011) Emerging phylogeographical patterns of plants and terrestrial vertebrates from Patagonia. *Biological Journal of the Linnean Society* 103: 475–494.
https://doi.org/10.1111/j.1095-8312.2011.01656.x

Söderström, L., Hagborg, A., von Konrat, M., Bartholomew-Began, S., Bell, D., Briscoe, L., Brown, E., Cargill, D.C., da Costa, D.P., Crandall-Stotler, B.J., Cooper, E., Dauphin, G., Engel, J., Feldberg, K., Glenny, D., Gradstein, S.R., He, X., Hentschel, J., Ilkiu-Borges, A.L., Katagiri, T., Konstantinova, N.A., Larraín, J., Long, D., Nebel, M., Pócs, T., Puche, F., Reiner-Drehwald, E., Renner, M., Sass-Gyarmati, A., Schäfer-Verwimp, A., Segarra-Moragues, J., Stotler, R.E., Sukkharak, P., Thiers, B., Uribe, J., Váňa, J., Wigginton, M., Zhang, L. & Zhu, R.L. (2016) World checklist of hornworts and liverworts. *PhytoKeys* 59: 1–828s.
https://doi.org/10.3897/phytokeys.59.6261

Stamatakis, A. (2006) RAxML-VI-HPC: Maximum Likelihood-based Phylogenetic Analyses with Thousands of Taxa and Mixed Models.

Bioinformatics 22: 2688–2690.
https://doi.org/10.1093/bioinformatics/btl446

Stech, M., Pfeiffer, T. & Frey, W. (2002) Chloroplast DNA relationship in palaeoaustral *Polytrichadelphus magellanicus* (Hedw.) Mitt. (Polytrichaceae, Bryopsida). Studies in austral temperate rain forest bryophytes 12. *Botanische Jahrbücher fur Systematik, Pflanzengeschichte und Pflanzengeographie* 124: 217–226.
https://doi.org/10.1127/0006-8152/2002/0124-0217

Stephani, F. (1911) Botanische Ergebnisse der schwedischen Expedition nach Patagonien und dem Feuerlande 1907–1909. II. *Die Lebermoose. Kungliga Svenska Vetenskapsakade- miens Handlingar* (n.ser.) 46 (9): 1–92

Stephani, F. (1916) Species hepaticarum 5. George & Cie, Genève & Bale. *Missouri Botanical Garden* 833–1008.
https://doi.org/10.5962/bhl.title.95494

Stuessy, T. F., Foland, K.A., Sutter, J.F., Sanders, R.W. & Silva, O.M. (1984) Botanical and Geological Significance of Potassium-Argon Dates from the Juan Fernández Islands. *Science* 225: 49–51.
https://doi.org/10.1126/science.225.4657.49

Spruce, R. (1885): Hepaticae of the Amazon and the Andes of Peru and Ecuador. Transactions and proceedings of the *Botanical Society of Edinburgh*. 15: 1–588.

Sun, Y., He, X. & Glenny, D. (2014) Transantarctic disjunctions in Schistochilaceae (Marchantiophyta) explained by early extinction events, post-Gondwanan radiations and palaeoclimatic changes. *Molecular Phylogenetics and Evolution* 76: 189–201.
https://doi.org/10.1016/j.ympev.2014.03.018

Swenson, U., Hill, R. & McLoughlin, S. (2001) Biogeography of *Nothofagus* supports the sequence of Gondwana break-up. *Taxon* 50: 1025–1041.
https://doi.org/10.2307/1224719

Swofford, D.L. (2001) PAUP*: phylogenetic analysis using parsimony, version 4.0. Smithsonian Institution, Washington, D.C.

Truswell, E. M. & Macphail, M. K. (2009) Polar forests on the edge of extinction: what does the fossil pollen and spore evidence from East Antarctica say? *Australian Systematic Botany* 22: 57–106.
https://doi.org/10.1071/SB08046

Vanderpoorten, A., Gradstein., S.R., Carine, M.A. & Devos, N. (2010) The ghosts of Gondwana and Laurasia in modern liverwort distributions. *Biological Reviews of the Cambridge Philosophical Society* 85: 471–487.
https://doi.org/10.1111/j.1469-185X.2009.00111.x

Vanderpoorten, A., Devos, N., Goffinet, B., Hardy, O.J. & Shaw, A.J. (2008) The barriers to oceanic island radiation in bryophytes: insights from the phylogeography of the moss *Grimmia montana*. *Journal of Biogeography* 35: 654–663.
https://doi.org/10.1111/j.1365-2699.2007.01802.x

Váňa, J. & Engel, J. (2013) The liverworts and hornworts of the Tristan da Cunha group of islands in the South Atlantic Ocean. *Memoirs of The New York Botanical Garden* 105: i–x, 1–137.

Vasconcelos, T.N.C., Proença, C.E.B., Ahmad, B., Aguilar, D.S., Aguilar, R., Amorim, B.S., Campbell, K., Costa, I.R., De-Carvalho, P.S., Faria, J.E.Q., Giaretta, A., Kooij, P.W., Lima, D.F., Mazine, F.F., Peguero, B., Prenner, G., Santos, M.F., Soewarto, J., Wingler, A. & Lucas, E.J. (2017) Myrteae phylogeny, calibration, biogeography and diversification patterns: increased understanding in the most species rich tribe of Myrtaceae. *Molecular Phylogenetic and Evolution* 109:113–137.
https://doi.org/10.1016/j.ympev.2017.01.002

Villarreal, J.C. & Renzaglia, K.S. (2006) Sporophyte structure in the neotropical hornwort *Phaeomegaceros fimbriatus*: implications for phylogeny, taxonomy and character evolution. *International Journal of Plant Sciences* 167: 413–427.
https://doi.org/10.1086/500995

Villarreal, J.C., Cargill, D.C., Hagborg, A., Söderström, L., & Renzaglia, K.S. (2010a) A synthesis of hornwort diversity: Patterns, causes and future work. *Phytotaxa* 9: 150–166.
https://doi.org/10.11646/phytotaxa.9.1.8

Villarreal, J.C., Cargill, D.C. & Goffinet, B. (2010b) *Phaeomegaceros squamuliger* subspecies *hasselii* (Dendrocerotaceae, Anthocerotophyta), a new taxon from the Southern Hemisphere. *Nova Hedwigia* 91: 349–360.
https://doi.org/10.1127/0029-5035/2010/0091-0349

Villarreal, J.C., Goffinet, B., Duff, R.J. & Cargill, D.C. (2010c) Phylogenetic delineation of the genera *Nothoceros* and *Megaceros*. *The Bryologist* 113: 106–113.
https://doi.org/10.1639/0007-2745-113.1.106

Villarreal, J.C. & Renner, S.S. (2013) Correlates of monoicy and dioicy in hornworts, the apparent sister group to vascular plants. *BMC Evolutionary Biology* 13: 239.
https://doi.org/10.1186/1471-2148-13-239

Villarreal, J.C. & Renner, S.S. (2014) A review of molecular clock calibrations and substitution rates in liverworts, mosses, and hornworts,

and a timeframe for a taxonomically cleaned-up genus *Nothoceros*. *Molecular Phylogenetics and Evolution* 78: 25–35.
https://doi.org/10.1016/j.ympev.2014.04.014

Villarreal, J.C., Cusimano, N. & Renner, S.S. (2015) Biogeography and diversification rates in hornworts: the limitations of diversification modelling. *Taxon* 64: 229–238.
https://doi.org/10.12705/642.7

Villarreal, J.C., Duckett, J.G. & Pressel, S. (2017) Morphology, ultrastructure and phylogenetic affinities of the single-island endemic *Anthoceros cristatus* Steph. (Ascension Island). *Journal of Bryology* 39: 226–234.
https://doi.org/10.1080/03736687.2017.1302153

Warnock, R.C.M., Yang, Z.H. & Donoghue, P.C.J. (2012) Exploring uncertainty in the calibration of the molecular clock. *Biology Letters* 8: 156–159.
https://doi.org/10.1098/rsbl.2011.0710

Yu, Y., Harris, A.J., Blair, C. & He, X.J. (2015) RASP (Reconstruct Ancestral State in Phylogenies): a tool for historical biogeography. *Molecular Phylogenetics and Evolution* 87: 46–49.
https://doi.org/10.1016/j.ympev.2015.03.008

Zapata, A., Rivera-Rondón, C.A., Valoyes, D., Muñoz-López, C.L., Mejía-Rocha, M., Catalan, J., 2021. Páramo lakes of Colombia: An overview of their geographical distribution and physicochemical characteristics. *Water* 13: 1–16.
https://doi.org/10.3390/w13162175
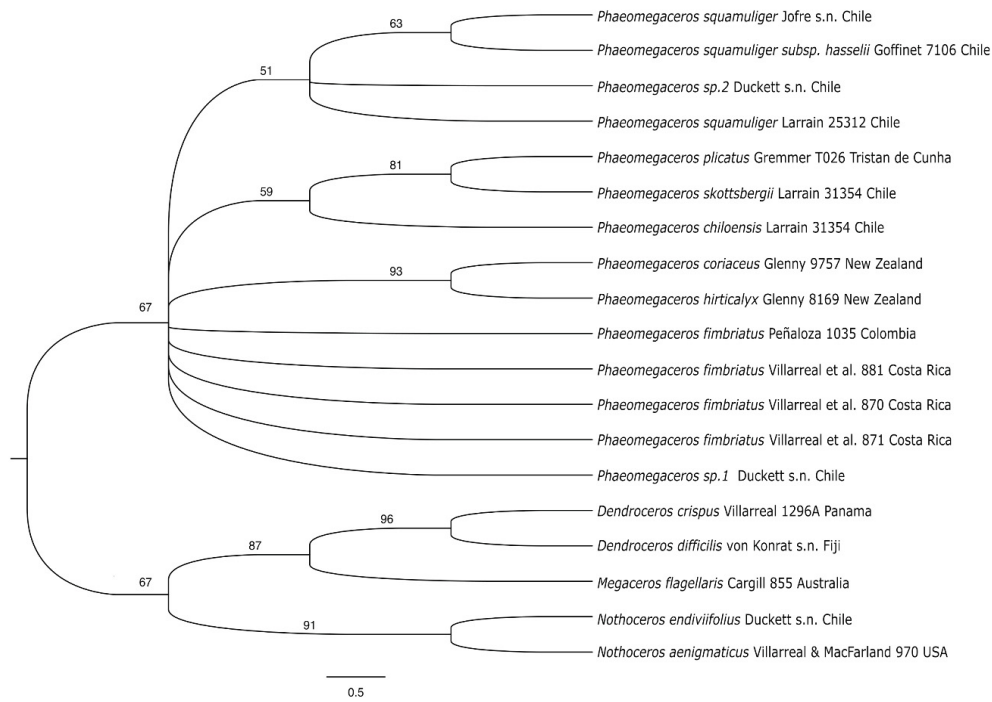
SUPPLEMENTAL FIGURE S1. Maximum likelihood majority rule consensus phylogenetic reconstruction of the genus *Phaeomegaceros* (Dendrocerotaceae) based on six chloroplast markers. ML bootstrap support is depicted on branches.
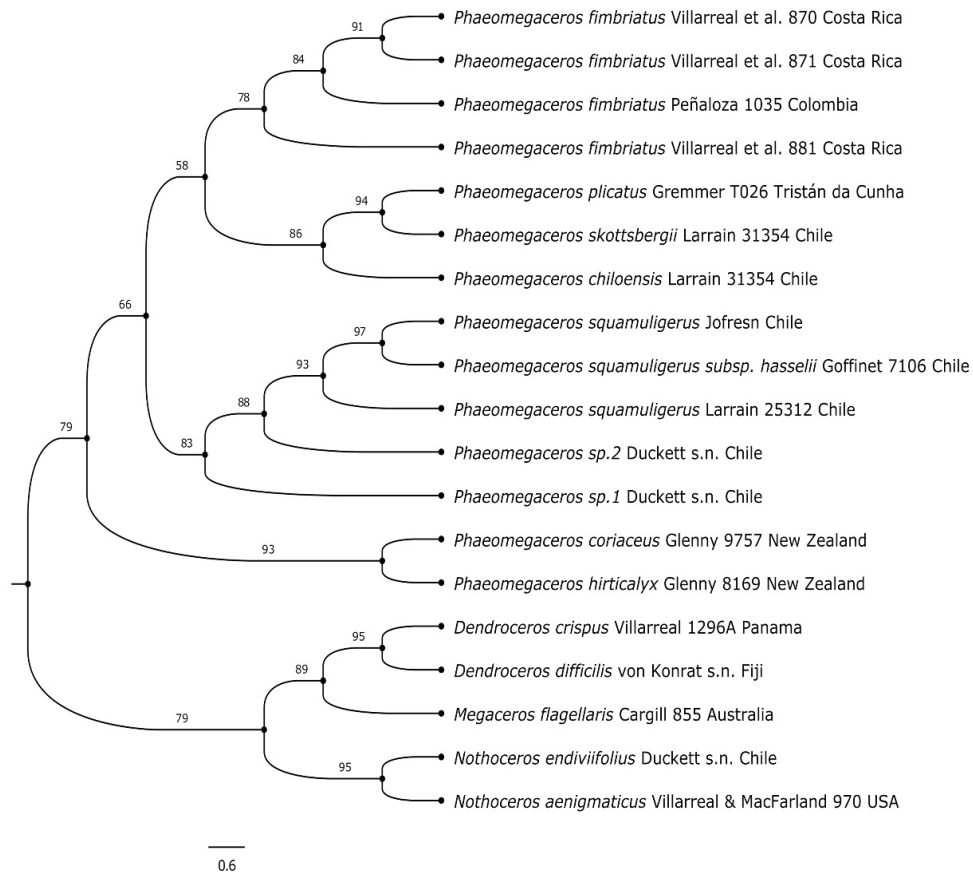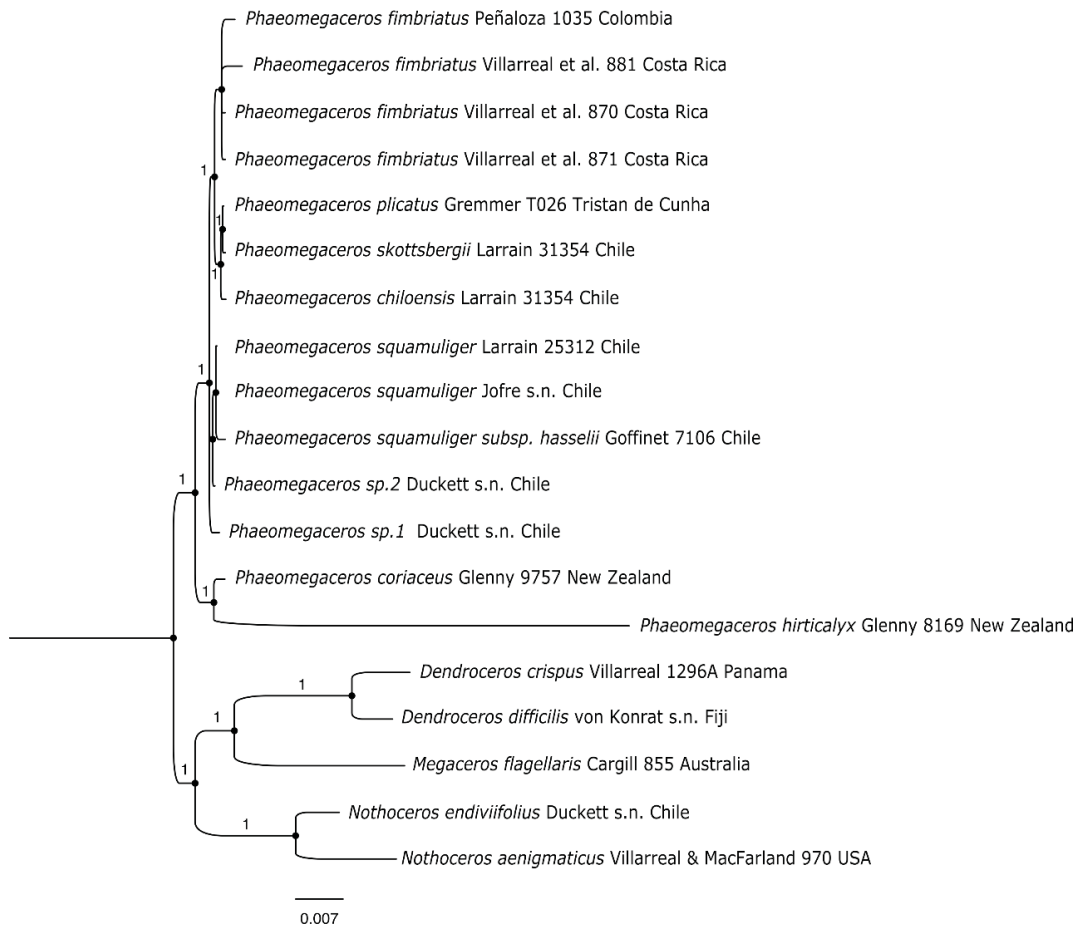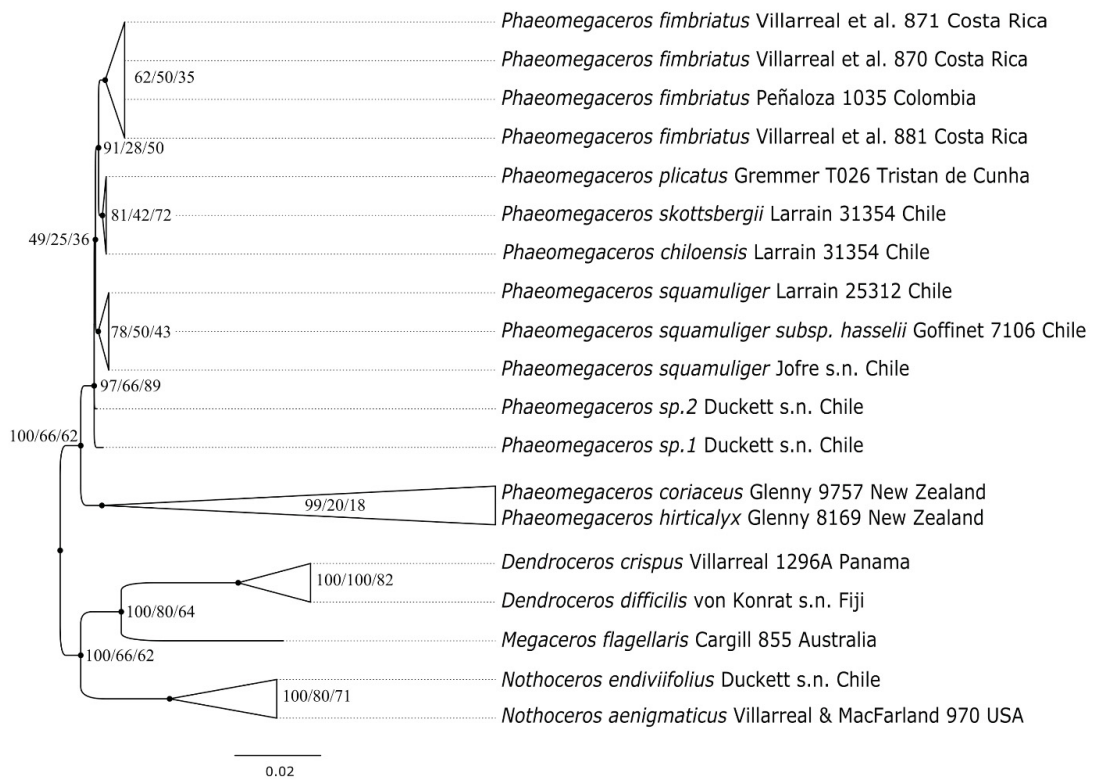

SUPPLEMENTAL FIGURE S2. Maximum likelihood majority rule consensus phylogenetic reconstruction of the genus *Phaeomegaceros* (Dendrocerotaceae) based on one nuclear, one mitochondrial and six chloroplast markers. ML bootstrap support is depicted on branches.

SUPPLEMENTAL FIGURE S3. Bayesian inference consensus tree of the genus *Phaeomegaceros* (Dendrocerotaceae) based on one nuclear, one mitochondrial, and six chloroplast markers. Bayesian posterior probability is depicted on branches.

SUPPLEMENTAL FIGURE S4. Maximum likelihood phylogenetic reconstruction of the genus *Phaeomegaceros* (Dendrocerotaceae) based on one nuclear, one mitochondrial, and six chloroplast markers. ML bootstrap values ≥75, gene concordance factor (gcf), and site concordance factor (scf) are depicted on branches, respectively.

SUPPLEMENTAL FILE 1: Morphological description of the populations of *P. fimbriatus* collected in the Paramos (above 3000 meters)

Phaeomegaceros fimbriatus (Gottsche) R.J. Duff, J.C. Villarreal, Cargill et Renzaglia, Bryologist 110 (2): 241, 2007.
≡*Anthoceros fimbriatus* Gottsche, Ann. Sci. Nat. Bot. (sér. 5) 1: 187, 1864.

Populations of *P. fimbriatus* collected in the Paramos (above 3000 meters) differed from other populations of *P. fimbriatus* from montane cloud forest by: **Thallus** dichotomously branched up to 32 mm long, broad 3–4 mm wide, narrower lobes in thallus growing crowded and almost upright. Thallus in cross-section (250) 400–700 (1000) μm thick, composed of 8–11 (20) cell layers; smooth dorsal surface, cuticle slightly thickened, brownish thallus margins; dorsal epidermal cells polygonal, 30–97.5 x 15–37.5 μm. **Chloroplast** single, dumbbell-shaped (9–40 x 5–23 μm), rarely two in the dorsal epidermis and smaller in inner cells, pyrenoid absent, ultra-structurally with a zonation of peripheral starch and granal stacks in the middle of the plastids. **Fungal** endophytes present in inner gametophyte cells, ventral clefts flanked by 2 cells. *Nostoc* colonies irregularly scattered on the ventral side, appearing as dark green to blackish dots. **Rhizoids** abundant, with darkish-purplish content and unbranched tips. **Dioicous**, male and female plants found intermixed or spatially segregate. **Androecium** single to 390 μm in diameter, irregular jacket cell arrangement, and a short stalk. **Involucres** erect, cylindrical, 1–2 (–4) mm, 9–13 cells wide in transverse section, smooth, slightly brownish at the mouth, and tightly appressed to the sporophyte. **Capsule** 1 per involucre, 42 mm long, with conspicuous longitudinal groove, opening by two valves, 700–1110 μm thick with 9–13 cell layers in transverse section, columella up to 30 cells; epidermal cells of the capsule rectangular to elongate 87–180 x 10–20 μm, thickenings along the outer free surface extending uniformly to the inner tangential walls; stomata 62–95 x 40–65 μm, abundant. **Spores** yellow, conspicuously vermiculate, individual vermiculae segmented, (45) 50–58 (–61) μm in diameter with 2–5 μm of cingulum, spores tetrahedral, occasionally may be slightly rectangular in equatorial view; the proximal face of spore with trilete mark developed, papilla-like projections abundant; the distal face of the spores with central fovea 1(–2), and 4–7(–9) around the periphery. **Pseudoelaters** 2–3 cells, 115–300 x 5–20 μm, slightly elongated, with slightly thick walls, interspersed with the spores, forming a three-dimensional mesh surrounding the tetrads.

Distribution and Habitat—These populations are restricted to soils in exposed areas, or close to water bodies in the Andean Páramos above 3200–4100 m; also found close to the crater of Volcan Irazú (ca. 3200 m) in Costa Rica, suggesting a restricted distribution to high altitude tropical areas.

Specimens Examined—COLOMBIA.—CALDAS DEPARTMENT: Volcán Ruiz, 4100 m. On wet, humose soil, July 1992, *Gradstein 9012*. COSTA RICA.—Volcán Irazú, area del crater 3200 m, 11 July 2006, *Villarreal, N. Wickett & Dauphin 871* (CONN!). ECUADOR.—NAPO PROVINCE: Cerro Sumaco, páramo, terrestrial, 3700-3800 m, 77°43' W; 00°34'S, May 1979, *Holm-Nielsen, J. Jaramillo & T. Vries, 17616.* (CANB!; Only sporophytes in this collection). VENEZUELA.—MÉRIDA: Páramo St. Domingo, 3900 m, 1999, *Gradstein & A. Berg 10008* (GOET!, MERC!); Sierra de Santo Domingo, Sierra Nevada National Park, Páramo de Mucubají. Banks of Río Mucubají, ca. 3 500 m. 10 January 2004, *M.J. Price 3500* (MERC!, G!, CONN!).

SUPPLEMENTAL TABLE S1. Specimens and sequences for each genetic marker information (Genbank accession number).

Species name	Extraction No.	collector no.	Locality	rbcL	nad5	trnL intron	trnL spacer	rps4 gene	rps4 spacer	matK	Phytochrome
Phaeomegaceros chiloensis	JC325	Larrain, 34061B	Chile	JX872449.1	JX872489.1	OQ129568	OQ129555	-	OQ129545	-	OQ129588
P. coriaceus	JC214	David Glenny, 9757	New Zealand	JX872450.1	JX872490.1	OQ129561	OQ129556	KP238750.1	OQ129554	KF482335.1	OQ129589
P. fimbriatus	JC036	Villarreal *et al.*, 870	Costa Rica	HM056149	-	OQ129562	-	OQ129571	OQ129546	-	-
P. fimbriatus	JC073	Villarreal *et al.*, 881	Costa Rica	OQ129541	OQ129578	HM067446	HM067497	KP238752.1	HM067548	JN559928.1	-
P. fimbriatus	JC037	Villarreal *et al.*, 871	Costa Rica	OQ129544	OQ129581	OQ129564	-	OQ129572	OQ129547	OQ129585	OQ129591
P. fimbriatus	JC2104	Peñaloza 1035	Colombia	OQ129539	OQ129579	OQ129570	-	OQ129577	-	OQ129587	-
P. hirticalyx	JC109	Glenny, 8169	New Zealand	-	-	OQ129569	-	-	OQ129552	OQ129584	-
P. plicatus	JC215	Gremmer, T026	Tristan da Cunha	OQ129540	OQ129580	OQ129563	OQ129557	KP238753.1	-	KF482337.1	OQ129590
P. skottsbergii	JC341	Larrain, 31354	Juan Fernández, Chile	OQ129542	-	OQ129565	OQ129558	KP238755.1	OQ129548	-	OQ129592
P. sp. nov. 1	JC354	Duckett, s.n.	Chile	DQ845656.1	DQ845714.1	OQ129566	OQ129559	OQ129573	OQ129549	OQ129586	-
P. sp. nov. 2	JC356	Duckett, s.n.	Chile	DQ845651	OQ129582	-	-	-	-	KF482339.1	-
P. squamuliger	JC130	Larrain, 25312	Chile	OQ129543	OQ129583	-	-	OQ129574	OQ129550	KF482340.1	OQ129594
P. squamuliger	JC132	Jofre, J., s.n.	Chile	HM038430	HM038432	OQ129567	OQ129560	OQ129575	OQ129551	-	OQ129593
P. squamuliger subsp. hasselii	JC236	Goffinet, 7106	Chile	HM038429	HM038431	-	-	KP238758.1	OQ129553	KF482341.1	OQ129595
Megaceros flagellaris	JC102	Cargill 855	Australia	HM056151	HM163392	HM067448	-	KP238713.1	HM067550	JN559929.1	-
Nothoceros endiviifolius	JC025	Duckett, s.n.	Chile	HM056152.1	HM163393.1	HM067449.1	-	HM163348.1	HM067551.1	JN559930.1	-
Nothoceros aenigmaticus	na	Villarreal & McFarland 970	USA	HM056194	HM163435	HM067491	-	OQ129576	HM067591	JN559969.1	-
Dendroceros difficilis	JC104	Von Konrat, s.n	Fiji	HM056148	JX872466.1	HM067445	-	KP238703.1	HM067547	JN559927.1	-
Dendroceros crispus	JC305	Villarreal 1296A	Panama	JX885633.1	KF482254.1	-	-	KP238702.1	-	KF482312.1	-

SUPPLEMENTAL TABLE S2. Diagnostic comparison of morphological characteristics between *P. fimbriatus* populations (Hässel de Menéndez 1989; Villarreal and Renzaglia 2006).

Taxon	*P. fimbriatus* collected in montane cloud forest	*P. fimbriatus* collected in Páramos
Thallus thickness (µm)	400-700	(250) 400-700 (-1000)
Thallus thickness (cells)	(7)8-16	ago/20
Dorsal outgrowths	Usually present	Absent
Stomata length and width (µm)	55-83 × 30-45	(54) 62-95 × (33) 40-65
Spore diameter (µm)	30-43	45-61
Distal spore ornamentation	(3) 5-7 foveas surrounding a central fovea. Sparsely vermiculate	(5) 6-9 foveas surrounding a central one (-2). Densely vermiculate
Proximal spore ornamentation	Nearly smooth surface with coarse verrucae	Vermiculate surface with small, scattered papilla-like processes

SUPPLEMENTAL TABLE S3. Summary of characters in the aligned nucleotide data by the separate marker.

	rbcL	*nad5*	*rps4 gene*	*rps4 spacer*	*trnL intron*	*trnL spacer*	*matK*	*Phytochrome*
Substitution model	GTR+I+Γ	GTR+I+Γ	GTR+Γ	GTR+Γ	GTR+Γ	GTR+I+Γ	GTR+I+Γ	GTR+I+Γ
Characters	1336	1094	551	465	582	577	1144	790
Constant	1213	1066	502	344	398	572	1040	776
Parsimony-uninformative	69	21	39	81	131	3	53	11
Parsimony-informative	54	7	10	40	53	2	51	3

SUPPLEMENTAL TABLE S4. Ancestral area reconstruction model with two-time slices indicating the probability of area connectivity assigned for the five major areas considered in the biogeographical reconstruction of *Phaeomegaceros*, based on reconstructed geological events (Estrella *et al.* 2019). The five major areas were assigned as follows: (A) New Zealand, (B) Southern-South America, (C) North, Central, and Northern-South America, (D) the Atlantic Island Tristan da Cunha, and (E) Antarctica.

1. Time slice: >30 Ma

	A	B	C	D	E
A	1	1	1	0.01	1
B	1	1	1	0.01	1
C	1	1	1	0.01	1
D	0.01	0.01	0.01	0.01	0.01
E	1	1	1	0.01	1

2. Time slice: 0-30 Ma

	A	B	C	D	E
A	1	0.5	0.5	0.01	0.5
B	0.5	1	1	0.01	0.5
C	0.5	1	1	0.01	0.5
D	0.01	0.01	0.01	0.01	0.01
E	0.5	0.5	0.5	0.01	0.5

SUPPLEMENTAL TABLE S5. Ancestral area reconstruction of the genus *Phaeomegaceros* without and with Antarctica as a Geographical Area. Event route and probability retrieved from biogeography reconstruction respective models are presented for each node. Number in clade column stands for the node age presented in Fig. 2. Different results on the event route are highlighted in bold. Bayesian posterior probability (BPP).

Node	Without antarctica	BPP	With antarctica	BPP
	Event route		Event route	
1	AB->B->BC->C|B	0.05	AE->AE^A->A|AE	0.39
2	C->AC->C|A	0.21	A->->^C->C^C->C|C	0.39
3	**B->AB->A|B**	**0.39**	**AE->ABE->AE|B**	**0.83**
4	**A->A^A->A|A**	**1**	**AE->AE^A^E->AE|AE**	**1**
5	**B->BC->B|C**	**0.77**	**B->B^B->B|B**	**0.84**
6	B->B^B->B|B	1	B->B^B->B|B	1
7	C->BC->C|B	0.83	B->BC->C|B	0.99
8	B->B^B->B|B	1	B->B^B->B|B	1
9	B->B^B->B|B	1	B->B^B->B|B	1
10	C->C^C->C|C	1	C->C^C->C|C	1
11	**B->BD->B|D**	**0.82**	**B->B^B->B|B**	**0.99**
12	D->BD->D|B	0.90	B->BD->D|B	0.99